Computer Simulation Study of The F^+ center in Magnesium Oxide

by

Ravindra Pandey

A thesis
presented to the University of Manitoba
in fulfillment of the
thesis requirement for the degree of
Doctor of Philosophy
in
Department of Physics

Winnipeg, Manitoba

ISBN 0-315-44156-9

COMPUTER SIMULATION STUDY OF THE F+ CENTER IN MAGNESIUM OXIDE

BY

RAVINDRA PANDEY

A thesis submitted to the Faculty of Graduate Studies of the University of Manitoba in partial fulfillment of the requirements of the degree of

DOCTOR OF PHILOSOPHY

I hereby declare that I am the sole author of this thesis.

I authorize the University of Manitoba to lend this thesis to other institutions or individuals for the purpose of scholarly research.

Ravindra Pandey

I further authorize the University of Manitoba to reproduce this thesis by photocopying or by other means, in total or in part, at the request of other institutions or individuals for the purpose of scholarly research.

Ravindra Pandey

ABSTRACT

The results of a detailed investigation of the ground and unrelaxed excited states of the F^+ center in magnesium oxide are presented. We use the program package, ICECAP, which allows self-consistent calculations to be made of the electronic structure and lattice distortion and polarization of a point-defect in an ionic crystal. The ground and unrelaxed excited states are shown to be well-localised. Spin density analysis illustrates the importance of basis set optimisation for nearest-neighbor ions and self-consistent lattice relaxation, yielding a good description of the ground state. Our calculation fails to give an acceptable value of the optical absorption energy, probably due to inadequate basis set optimisation of near-neighbor ions in the unrelaxed excited state. However the results reveal that second nearest-neighbor oxygen ions play an important role in the optical absorption process, and must be included in the defect cluster describing the unrelaxed excited state of the F^+ center in maganesium oxide.

ACKNOWLEDGEMENTS

I wish to express my sincere gratitude to Prof. J. M. Vail for his guidance and encouragement throughout the course of this work.

I am also indebted to Dr. A.H. Harker and Dr. J. H. Harding of AERE Harwell, England and Dr. C. Woodward and Dr. P. B. Keegstra of Michigan Technological University, Houghton, USA for numerous discussions and correspondences. These have contributed much to my understanding of localised electronic defect calculations in ionic crystals. I am particularly thankful to Dr. A. M. Stoneham and Prof. A. B. Kunz for hospitality and provision of computer facilities during my visits to AERE Harwell and Michigan Technological University, Houghton respectively.

We are grateful to Mr. B. Reid and Ms. K. Norman of the University of Manitoba computer center for facilitating the region size of about 5 Mbytes to execute the ICECAP load module and the disk space to store both the program package (400T) and integral files (3000T). We also acknowledge the generosity of Dr. R. Roshko and Dr. P. Loly, our departmental computer representatives, in feeding the ever-increasing appetite of computer units for ICECAP calculations.

This work has been supported in part by the Natural Science and Engineering Research Council of Canada through operating grants to Prof. Vail, and by the University of Manitoba Graduate Faculty through the award of a graduate fellowship to the author.

CONTENTS

Chapter I

GENERAL INTRODUCTION

1.1 INTRODUCTION

The computer-based microscopic description of the structure and properties of materials is an area of much current interest. Advances in computational and theoretical approaches have developed capabilities of yielding precise results and making succesful predictions. In coordination with current advances in experimental techniques, these theoretical efforts serve to elucidate complex processes and phenomena connected with the microstructure of materials. For example, computation of electronic structure can follow solid state processes at the atomic level in a degree of detail that the experimentalists would dearly love to observe but usually cannot. At the same time, it yields extra information about the properties such as bonding through the wavefunctions which can contribute to an understanding of the results obtained.

Ionic crystals make up a particular class of solid materials, characterized both by a marked localisation of electrons and strong insulating properties. A variety of thermal or chemical treatments or irradiations easily create

the so called 'point-defects', namely vacancies, interstitials, and impurities in the crystalline lattice of these materials. Since properties as diverse as mechanical strength or color are controlled by the point-defects, the nature of these point-defects has been of fundamental and practical concern for years.

During the past decade, there has been considerable growth in the use of computer simulation methods to study a diverse range of point-defect properties, including thermodynamic, structural and transport properties in ionic crystals. In particular, the development by Norgett[Norg 74] of a generalised computer program HADES(Harwell Automatic Defect Examination System) has led to a number of notable successes in yielding reliable quantitative values for the fundamental atomistic parameters such as, defect formation energies controlling transport properties in ionic crystals[Mack 82 and references therein].

HADES is based on a classical model which describes a crystalline lattice containing a point-defect as a set of point-ions, interacting by pair-wise potentials. However, the pairwise interaction between the ions near a defect will not be exactly the same as that in a perfect crystalline environment, from which the potentials are derived. Since this deviation depends sensitively on the detailed electronic structure near the defect, it is a quantum-

mechanical effect. Furthermore, the defect may be an intrinsically electronic defect such as, an electron trapped in a vacancy whose properties can only be understood on the basis of a detailed quantum-electronic structure analysis. It is therefore necessary to consider the electronic structure for both the defect and the ions immediately surrounding the defect from a quantum-mechanical point of view.

Assuming that the electronic structure effects of the defect are localised, the so called 'cluster approximation' [KK 78] can provide an effective model for point-defects in ionic crystals. In this approximation, the defect and its near vicinity can be considered as a many electron quantum-mechanical molecular cluster, representing an explicit region of the crystal in real space. A variety of molecular orbital methods can then be applied within this cluster to examine its electronic structure and properties. (For a general discussion we refer to HRSP 86, Ston 75). Convenient computer program packages are widely available for such molecular cluster calculations.

The major diffculty associated with the cluster approximation is the correct representation of the remainder of the crystal, since we are not dealing with an isolated 'super-molecule' but are attempting to simulate an infinite crystalline lattice. It is therefore necessary to add

features to the cluster approximation, and different boundary conditions have been proposed to provide the correct crystalline environment according to the nature of the problem under investigation.

For ionic crystals, particular care is needed to simulate the crystalline environment surrounding the cluster. A common approach is to combine the cluster approximation with a classical treatment of the crystalline environment. The cluster is generally embedded in a large array of point-charges, representing the crystalline environment. The positions and magnitudes of these point-charges are now varied to simulate the crystal potential in a reasonable way. This approach has been widely adopted in studying the point-defects in ionic crystals, for example, self-trapped exciton in NaCl[Ston 74], H chemisorption on NiO[WSWK 80], and the F center in LiF[TM 81].

Recently, Vail et al.[VHHS 84] have described a method, combining a quantum-mechanical treatment of ions near a point-defect in an ionic crystal with self-consistent polarization in the surrounding perfect lattice. In this method, the defect cluster is treated in the unrestricted Hartree-Fock self-consistent field (UHF-SCF) approximation and the surrounding lattice is described in terms of the shell model. Minimising the total energy of the defect cluster plus surrounding lattice with respect to variation

of cluster ionic positions, and simultaneously maintaining multipole consistency between cluster and surrounding lattice then leads to a physically consistent solution. Vail et al. have applied this method to the point-defect, F^+ center in magnesium oxide. The results show qualitative agreement with experiment and have cast considerable light on the role of lattice polarization and the details of the electronic structure of the ions neighboring the defect (that is, the ion-size effect) in accurate calculations of the optical absorption and emission of the F^+ center in magnesium oxide.

In an ionic crystal, the electronic structure of the ion is assumed to be well localised about the nuclei. However in the work of Vail et al., it was seen that the defect cluster wavefunction has a tendency to delocalise unphysically compared to true crystalline behaviour when embedded in a classical point-ion lattice. This may be due to the fact that the Coulomb field of the surrounding classical lattice does not force localisation upon the defect cluster of quantum-mechanical origin. Thus, some treatement less detailed than UHF-SCF approximation such as associating a pseudopotential, has been suggested for ions surrounding the defect cluster. Furthermore, a need for an automation of this procedure in the form of a well-documented, user-friendly program package to perform calculations for wide range of materials and defect types has been recognised [Vail 85].

The development of a generalised, automated program package, ICECAP (Ionic Crystal with Electronic Cluster : Automated Program), to provide a physically reliable model in a convenient and efficient computational form for analysing point-defects in ionic crystals, provides a base for this thesis work.

ICECAP is based on the HADES-shell model treatment of the embedding lattice[Norg 74], incorporating a UHF-SCF molecular cluster approximation[KK 78] of the defect and its near vicinity. It allows for electrostatic consistency up to octupole order between the cluster and the embedding lattice. It provides the cluster boundary conditions in the sense of approximate orthogonalisation of cluster to lattice either by associating pseudopotentials[TMM$^+$ 76, BHS 82] with a cage of cations surrounding the cluster or introducing a consistent localised potential(KKLP) for ions in the vicinity of the cluster into Fock operator[KV]. Electronic correlation can be introduced in terms of many-body perturbation theory[Kunz 83].

1.2 STRUCTURE OF THIS THESIS

In this thesis, the theoretical background of ICECAP is given in Chapter 2. This includes the description of HADES-shell model, UHF-SCF approximation, pseudopotentials and KKLP procedure. The program package and its numerical implementation are described in Chapter 3.

Since both the ICECAP code, and the model upon which it is based are relatively new and not extensively tested, the point-defect, F^+ center in magnesium oxide has been chosen to test the operation of the program plus its options and the physical accuracy of the model. The results of a detailed investigation of the ground and unrelaxed excited states of this defect are presented in Chapter 4. Also the conclusions drawn from the work are summarised and some suggestions are made for future work.

Chapter II

THEORETICAL BACKGROUND

2.1 INTRODUCTION

Point-defects in ionic crystals may be viewed theoretically as consisting of two regions, namely an inner region in the immediate vicinity of the defect where deviations from perfect lattice conditions can only be determined by quantum mechanical analysis, and the outer region for which the perturbation due to the defect is weak and to which a classical model successful in describing weak perturbations of the perfect crystal may be applied.

The defect and its immediate vicinity may be treated as a molecular cluster of ions for which ICECAP uses the program package, developed by Kunz and coworkers[Kunz]. This program package implements the unrestricted Hartree-Fock self-consistent field (UHF-SCF) approximation and provides pseudopotentials as options for ionic cores in the cluster. The surrounding lattice is treated by HADES using the shell model and the Mott-Littleton method.

In this chapter, we describe briefly the shell model, HADES and the UHF-SCF approximation. Cluster boundary

conditions to be applied in interfacing quantum-mechanical and classical regions of the model defect lattice in a physically consistent and computationally practical way are also discussed.

2.2 THE EMBEDDING LATTICE

Ionic crystals can be described as an assembly of polarizable point-ions in the two-body central-force model, in which the total potential energy, $V(\underline{r}_1,\underline{r}_2,,,\underline{r}_N)$ of an assembly of N ions with coordinates $\underline{r}_1,,,,\underline{r}_N$ is written as

$$V(\underline{r}_1,\underline{r}_2,,,\underline{r}_N) = \sum_{i>j} V_{ij}(\underline{r}_i - \underline{r}_j) \qquad (2.2.1)$$

Thus, V is taken as a sum of pair interaction terms each of which is dependent only on the distance between the ions. These pairwise interactions can be written as the sum of long-range Coulomb interactions and short-range interactions. The latter describe the effects of interacting (electron) charge clouds of the neighboring ions.

It is assumed that short-range interactions can be represented by a simple analytical expression and the most widely used is due to Born and Mayer, which has the form

$$V(r) = A \exp(-r/\rho) \qquad (2.2.2)$$

This may be supplemented by short-range attractive terms, namely terms in r^{-6} and r^{-8}. In this expression, r is the distance between the ith and jth ions and the A and ρ are empirically determined parameters. These parameters are generally derived from empirical fitting to perfect lattice properties such as cohesive energy, elastic constants and dielectric constants, ensuring that the potential V, is compatible with lattice stability.

An alternative, non-empirical approach is to obtain the potential by electron gas methods(for example, Wede 67). Here, the interaction between charge densities representing the interacting ions are calculated, the densities being obtained by calculating the wavefunction of the isolated ion with an assumption about the crystalline environment. (For a general discussion, see CDM 82). Recently, an ab-initio method has been used to determine the potential between anions in magnesium oxide[HH 85]. Both, empirical and non-empirical types of parameterisation have been applied successfully to a wide range of ionic and semi-ionic crystals and compilations of these potentials are available[Ston 81, CKM 81].

Ionic polarization, that is, the response of the crystal to the electrostatic perturbation provided by a charged point-defect, can be simulated simply and effectively using the shell model[DO 58]. This model was originally developed

for describing lattice dynamics of ionic crystals, but is now most widely used in defect-simulation studies. In the shell model, each point-ion consists of a core of charge X and a shell of charge of Y, such that the total ionic charge Z is the sum of core and shell charges. The core and shell of a given ion are coupled by a spring with a force constant K, while the polarization energy is assumed to be an harmonic function of the core-shell separation. Since the mass of the ion is centered at the core, shells are essentially massless, and respond instantly and adiabatically to the electrostatic field. The relative displacement of core and shell gives a dipole moment associated with each ion. The polarizability of the ion α, is then given by $\alpha=Y^2/K$. The parameters Y and K are obtained by fitting to appropriate lattice properties such as the dielectric and elastic constants and phonon frequencies.

The cores and shells are treated as independent entities, referred to as species. Coulombic interactions apply between all species with the exception of the core and shell of the same ion. Non-Coulombic short-range interactions between adjacent ions are assumed to be shell-shell interactions, that is, the short-range interaction is determined primarily by that part of the electronic distribution which displaces during polarization.

The shell model allows us to simulate the dielectric properties of the crystal accurately. It also provides adequate agreement on fitting to experimental phonon dispersion curves. A few discrepancies, however, occur which are due largely to the intrinsic inadequacies of the central-force approximation. The most important one is that the shell model cannot predict the Cauchy violation in the cubic crystals; that is, the model will predict that the elastic constants C_{12} and C_{44} are equal at 0^0K, although they can be significantly different, as is the case in magnesium oxide. Subsequently, refinements in the shell model have been proposed by introducing 'breathing shells' which allow spherically symmetric and ellipsoidal distortion of the shells and thus reproduce the Cauchy violation[Sang 74]. However, it is to be noted here that the calculated defect-energies have been found insensitive to a particular choice of shell parameters as long as they reproduce the bulk dielectric behavior of the crystal[CN 73, MS 79].

2.2.1 HADES

HADES, the Harwell Automatic Defect Examination System, is a computer program package for the calculation of point-defect energies and the lattice distortions introduced by such defects in ionic crystals. Much of the general theory underlying the program package has been developed from the Mott-Littleton approximation[ML 38] and has been described in various reports[Norg 74, Norg 77, CJMS 82].

The basic method divides a crystalline lattice containing the defect into two regions:

(a) An inner region(region I) is defined consisting of the defect and its immediate vicinity. In this region, the ions interact according to the shell model and the lattice configuration is evaluated explicitly by relaxing each ion until it is subject to no force.

(b) The outer region(region II) represents the rest of the lattice and is weakly perturbed by the defect. The lattice distortion in this region is calculated by considering the lattice as a dielectric continuum so that the ions are displaced in response to the effective charge of the defect.

In this approximation, the total lattice energy may be written as :

$$E(\underline{X},\underline{Y}) = E_1(\underline{X}) + E_{12}(\underline{X},\underline{Y}) + E_2(\underline{Y}) \qquad (2.2.3)$$

where, $E_1(\underline{X})$ is the energy of the inner region I expressed as a function of the ionic coordinates $\underline{X}$, $E_2(\underline{Y})$ is the energy of region II as a function of the ionic displacements $\underline{Y}$ and $E_{12}(\underline{X},\underline{Y})$ is the interaction energy between the two regions.

Now, it is assumed

(i) that $E_2(\underline{Y})$ is a quadratic function of the displacements in region II,

$$E_2(Y) = \frac{1}{2}\ \underline{Y}.\underline{\underline{A}}.\underline{Y}$$

(2.2.4)

where $\underline{\underline{A}}$ is the force-constant matrix of the perfect crystal. (ii) that the equilibrium condition for $\underline{Y}$ is

$$\left.\frac{\partial E}{\partial \underline{Y}}\right|_{\underline{y}=\underline{y}'} = 0 \qquad (2.2.5)$$

in which $\underline{Y}'$ are the equilibrium values corresponding to arbitrary values of $\underline{X}$.

The total energy, E then becomes

$$E(\underline{X},\underline{Y}') = E_1(\underline{X}) + E_{12}(\underline{X},\underline{Y}') - \frac{1}{2}\left.\frac{\partial E_{12}}{\partial \underline{Y}}\right|_{\underline{y}=\underline{y}'} \cdot \underline{Y}' \qquad (2.2.6)$$

This expression now involves interactions only between ions within region I and between those in regions I and II; all interactions between ions in region II are eliminated.

At this point, it is necessary to introduce a further approximation since the summation of the interactions of all pairs of ions between region I and region II, contributing to energy E_{12} is diffcult to evaluate as region II extends to infinity. Since the energy E_{12} is a sum of two contributions, namely Coulombic and non-Coulombic, it is assumed that the contribution due to the latter has a maximum range. Beyond this range, the contribution to E_{12} from region II is purely Coulombic. In other words, region II is itself sub-divided. Region IIa, surrounding the

region I is defined in which short-range non-Coulombic interactions between the displaced ions and those in region I is explicitly calculated. The outer region IIb is treated as a continuum assuming that the displacements in this region are purely a dielectric response to the effective charge of the defect. (For further details, we refer to Lidiard and Norgett[LN 72]).

In the total energy expression(2.2.6), the short-range non-Coulombic part is thus simply summed explicitly over a finite region of real space. For the Coulombic part, the aim is to modify the summation so that interactions between explicit ions in region I can be excluded. This is achieved by the Ewald method which replaces a point-charge by a Gaussian charge distribution. The complete lattice sums are then evaluated in real space and the explicit terms for inner region I are subtracted by transforming and performing a rapidly convergent reciprocal lattice space summation. The method in detail is described by Norgett[Norg 74].

As discussed earlier, the equilibrium configuration in region I is determined by requiring that the force on each ion is zero, that is,

$$\frac{\partial E}{\partial \underline{X}} \Big|_{\underline{Y}=\underline{Y}'} = 0 \qquad (2.2.9)$$

Solution of this equation requires $\underline{Y}$ to be constant. But since the displacements in region II can vary significantly

during minimisation, $\underline{Y}$ is updated between successive iterations.

In order to describe the crystal lattice in this region I/region II formulation, HADES requires as input data, the lattice vectors, unit cell components, the defect configuration and sizes of region I and IIa, to generate all the lattice sites within a given radius from the defined defect-origin. Since the symmetry of any defect must be equal or lower than the symmetry of the unit cell of the perfect lattice, HADES starts with the symmetry operations of either cubic or hexagonal point-group and defines the defect symmetry from the given initial defect configuration. Using this symmetry, defects and lattice sites are sorted into classes of sites equivalent by symmetry, thereby reducing the crystal region to a minimum number of independent variables. Finally, HADES identifies interactions between groups of ions that are equivalent so that it evaluates a single energy for each class of equivalent interactions together with an appropriate weighting factor, which corresponds to the number of ions in the respective classes. Thus, HADES accelerates the calculation by exploiting symmetry to reduce the number of variables to be used in minimisation.

The minimisation method used in HADES is a second-derivative type and requires the storage and inversion of

the second-derivative matrix. The inverse second-derivative matrix is only calculated once and afterwards updated at intervals. The following sequence is employed for minimisation of the total energy in HADES :

(a) Since the lattice is in stable equilibrium, the perfect lattice second-derivative matrix, $W^{(0)}$ is easy to calculate. This matrix is now inverted and a first displacement, δ is calculated as :

$$\delta = - H^{(0)} g^{(0)}$$

where $H^{(0)}$ is the inverse second-derivative matrix and $g^{(0)}$ is the first-derivative vector.

(b) An improved approximation to the equilibrium configuration is obtained,

$$X^{(1)} = X^{(0)} - H^{(0)} g^{(0)}$$

and a new set of first-derivatives, $g^{(1)}$ is calculated.

(c) The second-derivative matrix, $H^{(0)}$ is now updated using one of the formulas that have been suggested by Fletcher[Flet 70].

(d) New coordinates are then obtained as

$$X^{(2)} = X^{(1)} - H^{(1)} g^{(1)}$$

and the cycle is repeated. The minimisation is successful when the largest component of the displacement is sufficiently small.

In summary, the success of the HADES-shell model method in describing perfect lattice harmonic properties as well as a wide range of non-electronic point-defect properties in

ionic crystals suggests that it should be valid in describing the effects of electronic point-defects in the embedded lattice region where electronic effects other than induced ionic dipole moments are negligible.

2.3 THE CLUSTER

The cluster is defined as consisting of the defect and its immediate vicinity in the crystal. A general formulation for its quantum-mechanical analysis can be given in terms of a Hamiltonian expressing all interactions present between electrons and nuclei within the cluster; the many-body Hamiltonian is :

$$H = He + Hn + Hi \tag{2.3.1}$$

where

$$He = \sum_i \left[-\tfrac{1}{2}\nabla_i^2 + \tfrac{1}{2}\sum_{i,j}{}' \frac{1}{|\underline{r}_i - \underline{r}_j|} \right] \tag{2.3.2}$$

$$Hn = \sum_I \left[-\frac{1}{2M_I}\nabla_I^2 + \frac{1}{2}\sum_{I,J}{}' \frac{Z_I Z_J}{|\underline{R}_I - \underline{R}_J|} \right] \tag{2.3.3}$$

$$Hi = \sum_i \sum_I \left[-\frac{Z_I}{|\underline{R}_I - \underline{r}_i|} \right] \tag{2.3.4}$$

in atomic units.

In this set of units, $\hbar$=1, e=1 and the electron mass=1. The

unit of energy is then the hartree(1 Hy = 27.21 eV) and that of distance is the bohr(1 bohr = 0.529 Å = 0.529×10^{-10} m).

The Schrodinger equation for the many-body wavefunction is:

$$H \Psi(\underline{r},\underline{R}) = E \Psi(\underline{r},\underline{R}) \qquad (2.3.5)$$

Here upper-case letters refer to nuclear properties and lower-case letters designate electronic properties. The Ith nucleus has atomic number Z_I, mass M_I, and position $\underline{R}_I$. The ith electron has a coordinate r_i, charge e and mass m_e.

All the physics of the system is contained in the solution of the Schrodinger equation(2.3.5) which in general is very cumbersome. In practice, it proves feasible to obtain approximate solutions. The method, either ab-initio or semiempirical[1] uses a number of simplifying assumptions and approximations that reduce the N-body problem to a N one-electron problem which is manageable. Many excellent articles on these methods are available in the literature, notably the ones by Reitz[Reit 55], and Lowdin[Lowd 55]. In the present work, the cluster is treated in the Hartree-Fock

[1] Ab-initio methods seek in principle exact solutions, implying that within the frame of a particular method no approximations are adopted; though the method itself is an approximation to the solution of the Schrodinger equation. All integrals appearing in the calculation are computed as exactly as numerically possible, whereas in semiempirical methods they are either neglected or approximated by simplified expressions and functions containing empirical parameters.

self-consistent field method which when coupled with systematic treatment of correlation is probably the most viable approximation to the exact solution of the quantum-mechanical many-body problem available today. We briefly outline this approximation in the following section.

2.3.1 Hartree-Fock Self-Consistent Field Theory

We begin with the Born-Oppenheimer approximation[BO 27] to decouple nuclear and electronic motion. This essentially amounts to neglecting phonon and dynamic electron correlation effects and reduces the problem of solving the Schrodinger equation(2.3.5) to that of an interacting-electron system in the field of a fixed nuclear potential corresponding to a static lattice.

The resulting N-electron Schrodinger equation,

$$[He + Hi]\Psi(\underline{r},\underline{R}) = E(\underline{R})\,\Psi(\underline{r},\underline{R}) \qquad (2.3.6)$$

then depends only parameterically on the nuclear coordinates $\underline{R}$. Exact solution of this equation can only be obtained in rather simple cases such as the hydrogen molecule; for systems with a large number of electrons the independent-particle or one-electron model[Hart 28] provides a method of approximate solution. According to this model, each electron sees, in addition to the potential of the fixed nuclei, only some average potential due to the charge distribution of the

other electrons and moves essentially independently throughout the system. The N-electron wavefunction(Ψ), a function of the space and spin coordinates of all the electrons taken together, can then be approximated as a product of one-electron functions that are known as spin orbitals, a term coined by Mulliken[Mull 32]. Since electrons are fermions, the N-electron wavefunction must satisfy the antisymmetry property to ensure that it obeys the Pauli principle.

Within the Hartree-Fock approximation[Fock 30], the N-electron wavefunction(Ψ), is represented by a single determinant whose elements are one-electron spin orbitals(Øs) and the orbitals are optimised to yield the best determinantal function according to the variational principle.

The determinantal form is known as a Slater determinant[Slat 30] and is given by

$$\Psi(\underline{r}_1, \underline{r}_2, \ldots \underline{r}_N) = \frac{1}{\sqrt{N!}} \begin{vmatrix} \phi_1(\underline{r}_1) & . & . & \phi_1(\underline{r}_N) \\ \phi_2(\underline{r}_1) & . & . & \phi_2(\underline{r}_N) \\ . & . & . & . \\ . & . & . & . \\ . & . & . & . \\ . & . & . & . \\ \phi_N(\underline{r}_1) & . & . & \phi_N(\underline{r}_N) \end{vmatrix}$$

(2.3.7)

This determinantal wavefunction is manifestly antisymmetric and accounts for the Pauli principle since the determinant vanishes unless the spin orbitals form a linearly independent set. The factor $(N!)^{-1/2}$ normalises the function in (2.3.7) when spin orbitals form an orthonormal set,

$$\int dr\ \phi i^{*}(\underline{r})\phi j(\underline{r}) = \delta_{ij}$$

(2.3.8)

We emphasise here that the choice of orthonormality of spin orbitals is a convenience and not a theoretical necessity. Furthermore,

$$\phi i(\underline{r}) = \phi_{i}(\underline{x})\,\chi_{i}(\sigma)$$

(2.3.9)

represents the 4-dimensional manifold of space($\underline{x}$) and spin(σ) coordinates of the spin orbitals concerned. We also assume in the following discussion that χ_s are normalised eigenfunctions of the z-component of the spin operator S; they may be labeled as 'spin-up' or 'spin-down', the two functions being mutually orthogonal. We also abbreviate combined integration over spin coordinates by integration over $\underline{r}$, that is,

$$\int dr = \sum_{\sigma} \int d\underline{x} \qquad (2.3.10)$$

In accordance with the variational principle, the expectation value of the Hamiltonian with antisymmetric normalized function (Ψ) is a rigourous upper bound to the exact energy, E of the system, that is,

$$\langle \Psi | H | \Psi \rangle = E' \geq E \qquad (2.3.11)$$

If the function (Ψ) happens to be the exact wavefunction for the electronic ground state, E' will be the exact energy E.

The variational principle may now be applied to determine the optimal orbitals in the determinantal function (Ψ) by adjusting (Øs) to minimise the energy E'. The resulting value of E' will then be as close to the exact energy E as possible. Hence, the best function (Ψ) is found by minimising E' with respect to (Øs). This implies the variational equations,

$$\frac{\partial E'}{\partial \phi_i} = 0 \qquad (2.3.12)$$

which leads directly to the equations, referred to as the Fock equations.

$$\langle H \rangle = \int dr\, \Psi^*(\underline{r})\, [He + Hi]\, \Psi(r)$$

$$= \sum_i \int d\underline{r}_1\, \phi_i^*(\underline{r}_1) \left[-\frac{1}{2} \nabla_i^2 - \sum_I \frac{Z_I}{|\underline{R}_I - \underline{r}_1|} \right] \phi_i(\underline{r}_1)$$

$$+ \frac{1}{2} \sum_i \sum_{i \neq j} \int d\underline{r}_1 \int d\underline{r}_2\, \phi_i^*(\underline{r}_1)\, \phi_j^*(\underline{r}_2)\, \frac{1}{|\underline{r}_1 - \underline{r}_2|}\, \phi_i(\underline{r}_1)\, \phi_j(\underline{r}_2)$$

$$- \frac{1}{2} \sum_i \sum_{i \neq j} \int d\underline{r}_1 \int d\underline{r}_2 \, \Phi_i^*(\underline{r}_1) \, \Phi_j^*(\underline{r}_2) \, \frac{1}{|\underline{r}_1 - \underline{r}_2|} \, \Phi_j(\underline{r}_1) \, \Phi_i(\underline{r}_2)$$

(2.3.13)

We introduce Lagrange multipliers λ_{ij} to maintain the orthonormality of the Øi during the variation :

$$\delta \left[< H > - \sum_i \sum_j \lambda_{ij} \left(\int d\underline{r}_1 \, \phi_i^*(\underline{r}_1) \phi_j(\underline{r}_1) \right) \right] = 0$$

(2.3.14)

At the stationary point, the integrand must be zero independent of $\delta \phi_i^*$ for every i, so

$$\left[- \frac{1}{2} \nabla_1^2 - \sum_I \frac{Z_I}{|\underline{R}_I - \underline{r}_1|} \right] \Phi_i(\underline{r}_1)$$

$$+ \frac{1}{2} \sum \int d\underline{r}_2 \, \Phi_j^*(\underline{r}_2) \frac{1}{|\underline{r}_1 - \underline{r}_2|} \Phi_j(\underline{r}_2) \, \Phi_i(\underline{r}_1)$$

$$- \frac{1}{2} \sum \int d\underline{r}_2 \, \Phi_j^*(\underline{r}_2) \frac{1}{|\underline{r}_1 - \underline{r}_2|} \Phi_j(\underline{r}_1) \, \Phi_i(\underline{r}_2)$$

$$= \sum_j \lambda_{ij} \Phi_j(\underline{r}_1)$$

(2.3.15)

The left side of (2.3.15) is the Fock operator applied to $\Phi_i(\underline{r}_1)$. Its first term represents the kinetic energy for the electron of coordinate $\underline{x}$, plus its potential energy in the field of all the nuclei. The second term represents the Coulomb potential energy acting on the electron at position $\underline{x}$ of all the electronic charge including that of the ith wavefunction and is called as the Coulomb integral J_{ij}. The

last term, referred to as the exchange term K_{ij}, takes account of antisymmetry, and for the fact that the electron does not act upon itself, which it would do if this term were absent. We may describe the combined effect of the exchange and Coulomb terms in the sense that electrons of opposite spins to the one under consideration produce an ordinary Coulomb potential, while for electrons of the same spin the Coulomb potential is not produced by the full charge distribution, but by a corrected one in which an amount of charge totalling one electron is removed from the immediate vicinity of the given electron. The region around each electron effectively excluded to electrons of the same spin is sometimes called the Fermi or exchange hole[Reit 55]. We may therefore express the Fock equation as the wave equation for a single electron, moving in the field produced by the nuclei and the average field of the remaining electrons. The average field consists of the field produced by electrons of opposite spin plus the field produced by electrons of the same spin but outside the Fermi hole.

The determinantal wavefunction will be unchanged under any unitary transformation, so we may choose that transformation which diagonalizes the matrix of Lagrange multipliers in (2.3.15). When the λ -matrix is diagonalised, the Fock equation becomes

$$F \, \phi_i(\underline{r}) = \epsilon_i \, \phi_i(\underline{r}) \qquad (2.3.16)$$

The eigenvalue ε_i , can be interpreted as the energy required to remove an electron from the ith orbital, within the framework of Koopman's theorem[Koop 33] assuming that all the remaining orbitals of the system are unaffected by the removal of the electron from ith orbital. Physically, the system is expected to readjust its orbitals to the new situation. Koopman's theorem is therefore valid only if such a readjustment or relaxation can be neglected. For real systems, it is usually found that Koopman's theorem gives a good approximation to the binding energy, although the relaxation effect is normally quite significant for the more tightly bound electrons.

The Fock equations are coupled, non-linear, integro-differential equations and therfore there is no direct method for solving them. In fact, each Fock equation requires prior knowledge of all the other orbitals. It is thus necessary to resort to a self-consistent field method(SCF) which consists, in principle, of initial more or less arbitrary selection of one electron orbitals. In this method, an initial Fock operator, say $F^{(0)}$, is calculated from some suitably chosen set of orbitals $\phi^{(0)}$. The eigenfunctions $\phi^{(1)}$ of $F^{(0)}$ are then used to construct a new operator $F^{(1)}$ whose eigenfunctions are $\phi^{(2)}$. This iterative cycle is continued until the solutions are self-consistent, that is, until the difference between two sets of orbitals in successive cycles of computation is sufficiently small to

achieve the desired accuracy. This general method of solution is called the HF-SCF method. The only constraints which have so far been described are that the orbitals are forced to be orthonormal, and functions of the space and spin coordinates of only one electron. This level of approximation is referred to as the generalised Hartree-Fock approximation(GHF) and has not yet been solved for any large system.

Given that the orbitals have the form, $\emptyset(\underline{r})=\phi(\underline{x})\,\chi\,(\sigma)$, one of the two most frequently made assumptions is that each orbital is required to be an eigenfunction of spin. In other words, $\emptyset(\underline{r})$ must be either $\phi(\underline{x})\alpha(\sigma)$ or $\phi(\underline{x})\beta(\sigma)$, where $\phi(\underline{x})$ represents the spatial part of the orbital and α and β corresponds to the spin-up and spin-down eigenfunctions of the spin operator Sz respectively. This constraint does not affect the form of the Fock equation and orthogonality of α and β ensures correct counting in the exchange integral. This mild constraint produces the level of approximation known as Unrestricted Hartree-Fock approximation(UHF). By way of contrast, the Restricted Hartree-Fock(RHF) approximation places an additional requirement on the orbital. For doubly occupied orbitals, the spin-up and spin-down spatial parts are required to be equal, unlike the UHF case. Therefore a RHF calculation produces orbitals which are eigenfunctions of both overall spatial symmetry and spin, which in turn may provide a quite incorrect

description of spin-density at a nucleus. The UHF calculation is free from this deficiency. Thus, RHF is useful in studying systems of high inherent symmetry whereas UHF finds increasing use in systems of the type under consideration in the present work.

The solution of the Fock equations by expanding molecular orbitals as a linear combination of atomic orbitals(LCAO) has been elegantly formulated by Roothaan[Root 60]. This formulation is the basis of the UHF-SCF program, used in the present work. Each one-electron molecular orbital is expressed as a LCAO, localised on the nuclear and other sites,

$$\emptyset i = \sum_{\mu} C_{\mu i}\, a_{\mu} \qquad (2.3.17)$$

where C_s are the molecular orbital expansion coefficients and a_s are sets of atomic orbitals.

The most frequently used forms for atomic orbitals are either Slater-type orbitals(STO) of the form, " $Nr^{n-1} \exp(-\alpha r) Y_l^m (\theta , \phi)$ " or Cartesian Gaussian-type orbitals(GTO) of the form, " $Nr^{n-1} \exp(-\alpha r^2) X^l Y^m Z^n$ " where the spherical harmonics are replaced by cubic harmonics[Boys 50]. The α's are a set of chosen exponents spanning a sufficiently wide range to give adequate flexibility for the determination of the orbitals in the variational calculation.

The STOs usually provide a rapidly convergent expansion for molecular orbitals. Because they possess a cusp at the nucleus, they lead to a good representation of the wavefunction near the nucleus. Unfortunately, multicentered integrals over STOs are quite diffcult to compute. On the other hand the strength of GTOs lies in the fact that multicentered integrals can be easily evaluated since the product of two gaussians on different centres is equivalent to a single gaussian on a new centre. However, the GTOs suffer from two major disadvantages. The first is the fact that the functions are steeper than the STOs and so inadequately describe outer regions of atoms and molecules. But, for solids, the correct atomic tail-shape is not helpful as bonding states are often built only awkwardly from STOs. The second disadvantage of GTOs is the lack of a cusp affecting the ability of gaussians to describe properties that rely on the wavefunction close to the nucleus. This may be overcome by using slightly larger expansions of GTOs. It is to be noted here that no one choice of basis functions has yet shown overall superiority[BW 72, CU 80].

There is growing preference towards GTOs over the STOs in atomic and molecular structure calculations because of the analyticity of multi-centered gaussian integrals, and availability of very efficient computer programs to handle this. The drawback is that many more of them have to be used

in order to achieve the same level of accuracy as, say, the double-zeta basis(a basis of two STOs per atomic orbital). The increase in the number of basis function corresponds to an increase N^4 in the number of integrals requiring evaluation, thereby leading to a considerable increase in computation time during the iterative solution. One way of reducing this problem is by the use of contracted sets of GTOs(CGTO). A CGTO is a linear combination of (primitive) Gaussians with fixed coefficients of the form

$$a_\mu = \sum_s d_{\mu s}\, g_s \qquad (2.3.18)$$

where n_c is the number of gaussians contracted to a single atomic orbital, d_s are the fixed contraction coefficients, and g_s are primitive gaussians. Provided the contraction coefficients are carefully chosen, the CGTOs are capable of giving results of comparable accuracy to their uncontracted counterpart[Whit 66]. The coefficients(d_s), for a wide variety of atoms and ions, have been computed and tabulated in the literature[Huzi 84].

We note here that an unpleasant technical feature, namely basis set superposition error, is associated with the HF-SCF procedure. The severity of it is proportional to the incompleteness of the atomic basis set. Thus, to the extent the atom-centered basis is inadequate, the HF-SCF procedure will attempt to utilise any available basis functions on

neighbouring centers to make up for the deficiency. No completely reliable scheme for either eliminating or estimating superposition errors has been given so far .

Calculations are performed in three steps. First, the labels generation program, LABELS, uses any available information on the symmetry of the given problem to generate a list of non-zero integrals to be computed. Then the polyatomic gaussian integrals evaluation program, POLYIN, evaluates the listed integrals. These two programs are from the Caltech POLYATOM program package[NBK+], as modified by Kunz and coworkers. POLYIN permits also the user to replace the core electrons of one or more atoms in the given problem with an effective potential or pseudopotential. Finally, the iterative program UHFABK of Kunz[Kunz] uses the integrals to form a self-consistent solution.

Knowledge of the wavefunction permits us to obtain an insight into the distribution of electrons in the molecular space and also into the various orbitals centered on each atom. This is achieved by the Mulliken population analysis[Mull 55] for the system under consideration by integrating the electron density over all space. (For a detailed discussion, we refer to HRSP 86). Such information is instrumental in analysis of charge transfer and determination of the character of the basis functions in the present work.

2.4 CLUSTER BOUNDARY CONDITIONS

When a quantum-mechanical cluster is embedded in a weakly perturbed classical lattice, there remains the question of achieving physical consistency, electrostatic and quantum-mechanical, between the cluster and the embedding lattice.

The embedded cluster is seen by the surrounding lattice as a Coulomb potential, computed from the quantum-mechanical charge density of the cluster itself. This Coulomb potential is expressed as a multipole expansion. Hence, electrostatic consistency (between the cluster and the embedding lattice) requires that the cluster simulators (a set of point-charges for simulating the cluster) that produce the lattice distortion $\underline{R}$ in the embedding lattice possess the same value of low-order electric multipole moments as does the quantum-mechanical cluster whose electronic configuration is determined by $\underline{R}$. The procedure adopted in ICECAP to achieve electrostatic consistency is described in Chapter 3.

Quantum-mechanical consistency, on the other hand, requires that the cluster boundary conditions reflect the quantum-mechanical structure of ions in the surrounding lattice. Since the embedding Shell-Model lattice does not provide any Pauli exclusion, the cluster wavefunction tends to spread unphysically compared to true crystalline behavior. It is therefore necessary to orthogonalise the cluster wavefunction to a realistic electronic crystalline environment.

It is impractical to significantly enlarge the size of the cluster since large clusters contain so many electrons that they exceed the maximum basis-set capacity and practical CPU time limitations of present Hartree-Fock programs. Hence, some treatment less detailed than the Hartree-Fock is required for ions at the cluster boundary. The well-known pseudopotential approach may be used by associating complete-ion pseudopotentials with ions that surround the cluster, to overcome these computational diffculties. Alternatively, we may use the formalism, proposed by Kunz and Klein[KK 78] which adds only one electron integrals and provides a systematic, mathematically rigourous boundary for the quantum-mechanical cluster. These steps would considerably enlarge the one-electron integral part of the calculation, but are much more efficient and manageable than a corresponding larger Hartree-Fock calculation.

Both the approaches, namely pseudopotential and Kunz-Klein orthogonalisation, have been included in ICECAP to provide appropriate cluster boundary conditions. We briefly describe their concept and construction methods in the following sections.

2.4.1 Pseudopotentials

A pseudopotential(≃ an effective potential) is an approximation to the real potential that an electron experiences in a solid and whose characteristic feature is its separation of core electrons properties from those of valence electrons. The atomic cores are composed of nuclei plus core electrons and are considered to be inert and unchanged in going from a gas of isolated atoms to a solid composed of strongly interacting atoms. It is assumed that the valence electrons are largely responsible for the bonding and most of the electronic properties commonly studied in chemistry and solid state physics.

Because the valence electron wavefunctions are orthogonal to the core electron states, they are repelled from the core region as a consequence of the Pauli exclusion principle. Philips and Kleinman[PK 59] demonstrated that this repulsive potential cancels a large part of the attractive Coulomb potential from the nucleus leaving a net weak pseudopotential. The basic idea of the pseudopotential method is then to take advantage of this orthogonality to simplify electronic structure calculations by eliminating the need to include atomic core states and the strong Coulombic potentials responsible for binding them.

Several methods have been developed to construct pseudopotentials and can be classified into two distinct categories :

(a) The so-called empirical pseudopotential method forces the pseudopotential to reproduce some experimentally determined features, such as reflectivity and density of states of the energy bands. The pseudopotential can then be used to compute a variety of properties and analyse experimental data. This method has been particularly successful in describing the band structures of semiconductors and simple metals. [For a general discussion, see Cohe 84 and references therein]

(b) Alternative approaches, relying more on 'first-principles', require only the atomic number as input to generate the atomic wavefunctions and a description of how the valence electrons interact with cores and among themselves, therby avoiding the introduction of empirical parameters. The basic assumption is the frozen-core approximation which pictures the cores as stationary when discussing the electron dynamics. The valence electrons are then solved self-consistently, orthogonalised to the frozen-core orbitals[PK 59]. The resulting pseudo-wavefunction approximates the true 'all- electron' wavefunction beyond the core radius and then extends smoothly inside the core. The pseudopotential responsible for generating the pseudo-wavefunction can then be used to compute a variety of properties[TMM$^+$ 76].

The ab-initio calculations to obtain pseudopotentials are, however, based on the Hartree-Fock calculations in which the radial equation for the wavefunction contains non-local exchange operator in the sense that each angular momentum component of the pseudo-wavefunction sees a different potential. This in turn complicates the problem of finding a local pseudopotential to replace the core. Goddard and coworkers[MG 74, MOG 74, TMM 78] have dealt with this complexity by introducing a pseudopotential basis set (powers of r times gaussian) and varying the coefficients to minimise the error in integrals of the non-local Schrodinger equation, satisfied by the pseudo-wavefunction. The resulting pseudopotential depends upon the angular momentum of the valence electron thereby reflecting particularly the different Pauli exclusion effects for different symmetries. It is of the form

$$V(\underline{R}) = \sum_{l=0}^{\infty} V_l(\underline{R}) \; |l><l| \tag{2.4.1}$$

where $|l><l| = \sum_{m=-l}^{+l} |lm><lm|$, a projection operator onto states of angular momentum l, and $V_l(\underline{R})$ is a radial funtion which can be expressed in terms of Gaussians :

$$V_l(\underline{R}) = \sum_K C_{kl} R^{n_k} \exp(-\gamma_{kl} R^2) \tag{2.4.2}$$

The resulting orbitals are called Core-less Hartree-Fock(CHF) orbitals. Since it is smoothly varying and has a

small amplitude in the core region, it does not require core-like basis functions. This allows minimisation of the number of basis functions required to give an accurate description of the eigenstates of the potential. A tabulation of the CHF pseudopotentials for atoms lithium to zinc is available[TMM+ 76]. In the present work, we refer to these CHF pseudopotentials as TOPIOL pseudopotentials.

The so-called orthogonality-hole problem, that is, the difference between the true electron density and the electron pseudo-density persists in the approaches following Philips-Kleinman[PK 59]. This results from the fact that the pseudo-wavefunction overestimates the electron charge inside the core region; forcing it to differ from the true valence wavefunction in amplitude, although it does have the same shape outside the core. When used in a self-consistent calculation, this error in amplitude is manifest in an incorrect Coulomb potential, and thus an incorrect distribution of charge[BHS 82].

Hamann et al[HSC 79] have introduced a new family of pseudopotentials, where a pseudo-wavefunction is nodeless and after normalisation it matches the true valence wavefunction beyond some core radius, say Rc. For a given pseudo-wavefunction, the radial Schrodinger equation is inverted to yield the corresponding pseudopotential. By construction the integrals from zero to R of the real and

pseudo charge agree for R > Rc for each valence state. The term 'norm-conserving' is used to describe pseudopotentials with these qualities, and it guarantees that the Coulomb potential produced, outside the core is identical for the real and pseudo charge distributions.

Bachelet et al[BHS 82] have developed a consistent set of norm-conserving pseudopotential for most of the periodic table. An ab-initio calculation via a density-functional approach [KS 65, SS 82] with the use of a local approximation for the exchange- and correlation- potential is performed[CA 80, PZ 81]. The numerical potentials are then constructed from energies, wavefunctions and potential of a reference full-core atom. Finally, analytical expressions are fitted to these numerical potential functions, yielding the total ionic pseudopotential :

$$V(\underline{r}) = \sum_{l} |l\rangle [\, V_l^{ion}(\underline{r}) + V_l^{so}(\underline{r})\, \underline{L}.\underline{S}\,] \langle l| \qquad (2.4.3)$$

where V_l^{so} is a difference potential describing the strength of spin-orbit coupling(relativistic correction) and is neglected in the present work. We may therefore express the pseudopotential as

$$V(\underline{r}) = V_{core}(\underline{r}) + \sum_{l=0}^{l_{max}} |l\rangle \Delta V_l^{ion} \langle l| \qquad (2.4.4)$$

where

$$V_{core}(\underline{r}) = -\frac{Z_v}{r} \sum_i C_i^{core} \exp\{(\alpha)^{1/2} r\} \qquad (2.4.5)$$

and

$$\Delta V_{l}^{ion}(\underline{r}) = \sum_{i=1}^{3} (A_i + r^2 A_{i+3}) \exp(-\alpha_i r^2) \qquad (2.4.6)$$

Each atom is thus characterised by (i) a valance charge Z_V and two sets of linear coefficients and decay constants describing the core, C_l^{core}, $\alpha_{2,i}$ i=1,2 respectively; (ii) for each l value, two sets of three linear coefficients each, A_i and A_{i+3}, corresponding to the decay constant α_i, i=1,2,3 for the average potential. A compilation is given of the parameters necessary to synthesize norm-conserving pseudopotentials for the elements hydrogen to plutonium [BHS 82] and in the present work, we refer to them as BHS pseudopotentials.

Woodward[Wood 85] has written and implemented efficient pseudopotential integral codes for both TOPIOL and BHS cases in the UHF$^+$ program package which we have used in the present work.

2.4.2 Kunz-Klein Localising Potential(KKLP)

Kunz and Klein have described a self-consistent procedure to include the interaction of an embedded cluster with its environment in cluster simulation studies[KK 78]. This procedure and its implementation in ICECAP is reviewed in some detail below. (For a general discussion, see KV).

Let us recall the generalised form of the Fock equation (2.3.16) :

$$F\phi_K = \epsilon_K \phi_K$$

where F is the Fock operator for the entire crystal. For systems under study, the Fock operator F can be divided into two parts; the first F_A , representing all interactions of the electrons with each other and with the nuclei within cluster(A), and the second U_A , representing the potential energy of interaction between the cluster(A) and its environment(E).

The cluster electrons(N_A) and the embedding lattice electrons(N_E) might be assumed to occupy separate manifolds of states, denoted k(A) and k(E) respectively. Since the crystalline lattice is made up of well-localised separate ions, the cluster electrons do not significantly overlap the manifold of the embedding lattice. However, basis sets for both cluster and embedding lattice are chosen subjectively, from physical insight, with the result that cluster and lattice do not occupy mutually exclusive manifolds of functions. In fact, the cluster manifold generally exceeds the occupied manifold(k(A)) in order to provide variational flexibilty. Thus, the cluster manifold contains both occupied and unoccupied(virtual) states of cluster electrons.

The Fock equation may now be written as

$$(F_A + U_A)\phi_K = \epsilon_K \phi_K \tag{2.4.7}$$

where

$$F_A = -\nabla^2 - 2\sum_{j(A)} Z_j |\underline{r}-\underline{R}_j|^{-1} + 2\int d\underline{r}' \, |\underline{r}-\underline{r}'|^{-1} \int d\underline{y} \, \delta(\underline{y}-\underline{r}')[1 - P(\underline{r},\underline{y})] \rho_A(\underline{r}',\underline{y})$$

and

$$U_A = -2\sum_{j(E)} Z_j |\underline{r}-\underline{R}_j|^{-1} + 2\int d\underline{r}' \, |\underline{r}-\underline{r}'|^{-1} \int d\underline{y} \, \delta(\underline{y} - \underline{r}')[1 - P(\underline{r},\underline{y})] \rho_E(\underline{r}',\underline{y}) \tag{2.4.8}$$

where $P(\underline{r},\underline{y})$ is the electron pairwise interchange operator and δ is the Dirac delta-function.

The Fock-Dirac one-electron density operator is given by,

$$\rho_A(\underline{r}',\underline{y}) = \sum_{K=1}^{N_A} \phi_K(\underline{r}') \, \phi_K(\underline{y}) \tag{2.4.9}$$

and similarly for ρ_E , with summations over k(E) from (N +1) to ∞ for an infinite crystal.

We note here that the Fock equation(2.4.7) for the cluster depends in part on the occupied states of the embedding lattice through U_A (since U_A depends on k(E) through ρ_E). However, we do not wish to solve for the states of the embedding lattice. On the other hand, if we choose them, then such a choice will generally not be orthogonal to the cluster manifold as the chosen k(E) states will at most be orthogonal to the occupied states and not to the unoccupied states of the cluster. Furthermore, if we decide to project k(E) out of k(A) then the projection may reduce k(A) from its original range in Fock space making incorrect evaluation of certain defect properties. On the other hand, the projection of k(A) out of k(E) may distort the effect of surrounding ions in the cluster. In fact, we would like to incorporate the orthonormality between our cluster and lattice manifolds maintainining our careful choice of both cluster and lattice basis sets.

This has been approached by applying a subsidary condition which modifies the Fock equation(2.4.7) by adding an arbitrary effective potential. The procedure, described by Gilbert[Gilb 64] is based on the fact that the density operator, ρ_A ($=\Sigma|k><k|$, where $|k>$ is the state vector corresponding to orbital ϕ_k) is a projection operator onto the manifold of occupied states(that is, $\rho_A^2 = \rho_A$ and $\rho_A = \rho_A^*$) with the property that

$$\rho_A|k> = |k>, \text{ if k is occupied}$$

$$= 0, \text{ if } k \text{ is unoccupied.}$$

(2.4.10)

An important consequence of this property is that the projection $(\varrho_A W \varrho_A)$ of an arbitrary one-electron operator W onto the manifold of occupied states(k(A)) will satisfy the equation :

$$\varrho_A W \varrho_A |k\rangle = W|k\rangle, \text{ if } k \text{ is ocuupied}$$
$$= 0, \text{ if } k \text{ is unocuupied.}$$

(2.4.11)

Since,

$$W|k\rangle = \sum_{j=1}^{N_A} Wjk|j\rangle + \sum_{j=(N_A+1)}^{\infty} Wj'k|j'\rangle$$

(2.4.12)

where $Wjk = \langle j|W|k\rangle$. We then have

$$\varrho_A W \varrho_A |k\rangle = \sum_{j=1}^{N_A} Wjk|j\rangle, \text{ if } |k\rangle \text{ is ocupied}$$
$$= 0, \text{ if } |k\rangle \text{ is unocupied.}$$

(2.4.13)

By adding together equations(2.4.7) and (2.4.13), we obtain

$$(F_A + U_A + \varrho_A W \varrho_A)|k\rangle = \sum_{j=1}^{N_A} (\mathcal{E}_j \delta_{jk} + Wjk)|j\rangle$$

(2.4.14)

which is structurally identical to the general Fock equation(2.4.7). A unitary transformation within the manifold of occupied states may then be sought to yield the diagonal form of a modifed HF equation for an arbitrary one-electron operator W. Thus,

$$(F_A + U_A + \varrho_A W \varrho_A)|k\rangle = \pi_k |k\rangle$$

$$\text{for } k = 1,2,\ldots.N_A \qquad (2.4.15)$$

Since the electronic density of the embedding lattice(k(E)) is well-localised about the nuclei in ionic crystals, we may divide the environmental contribution U_A into long-range Madelung(or Coulomb) contribution, V_A^M, and short-range contribution, V_A^S. The Madelung term, arising from point-charge ions is given by

$$V_A^M = -2 \sum_{j(E)} I_j |(\underline{r}-\underline{R}_j)|^{-1} \qquad (2.4.16)$$

in atomic (Bohr-Hartree) units. Here, $I_j = (Z_j - N_j)$ and $\underline{R}_j$ are ionic charges and positions respectively, and N_j is the number of electrons associated with the ion j with E designating for ions outside the cluster.

The short-range term (V_A^S) is the potential arising from the electrons in the occupied orbitals of the environment and is given by

$$V_A^S = -2 \sum_{j(E)} N_j |\underline{r}-\underline{R}_j|^{-1} + 2 \int d\underline{r}' |\underline{r}-\underline{r}'|^{-1} \int d\underline{y}\ \delta(\underline{y}-\underline{r}')[1 - P(\underline{r},\underline{y})]\ \rho_E(\underline{r}',\underline{y}) \qquad (2.4.17)$$

In the modified Fock equation(2.4.15), the one-electron operator W, is taken equal to $-V_A^S$, so that

$$(F_A + V_A^M + V_A^S - \rho_A V_A^S \rho_A)|k> = \varepsilon_k |k> \qquad (2.4.18)$$

The added effective potential($-\ell_A V_A^S \ell_A$) is the Kunz-Klein localising potential and in the limit of self-consistency, it cancels out the V_A^S, the short range potential due to lattice ions as seen by cluster electrons. The equation(2.4.18) then reduces to :

$$(F_A + V_A^M) |k> = \pi_k |k>$$

(2.4.19)

Thus, it is in this sense that KKLP is a localising potential, because the cluster electrons end up seeing lattice ions as weakly perturbed point charges, and the essence of orthogonalisation without compromising either cluster or lattice basis sets has been captured by KKLP. The appropriate total-energy algorithm for equation(2.4.18) has been given by Kunz and Vail[KV].

In practice, the orbitals in the environment are obtained from solutions to the equation(2.4.18) for the perfect crystal. The KKLPs localised about individual ions in the environment are derived for each species in a perfect crystal and are then associated with those ions that neighbor a defect cluster. The use of perfect-lattice KKLPs with a defect cluster is consistent with the idea that the cluster should contain all significant deviations from perfect-lattice electronic structure.

The short-range potential(V_A^S) may be considered to be made up of additive contributions from all the ions in the

environment. It falls off very rapidly with distance, and so only contributions from ions in the immediate vicinity of the cluster need to be considered. We use Kunz's LOPAS code[Kunz], which solves the modified Fock equation(2.4.18) for each ionic species in a perfect lattice, with V including only a few sets of near-neighbors. A set of orbitals is associated with each ionic species which are taken to be linear combinations of Slater-type orbitals in our case from Clementi and Roetti[CR 74] and consistency is obtained between the two species. This solution is then used to determine KKLP for each species using Keegstra's KKLFIT code[Keeg 86] . Here, KKLP is evaluated on a grid of positions and then fitted to a set of gaussians, since evaluation of integrals is only possible in the POLYIN subroutine of ICECAP in terms of gaussians. The result is a set of localising potentials, one for each ionic species, which can be added at as many ionic sites of the embedding lattice as desired in equation(2.4.18). In contrast with the use of tabulated pseudopotentials(TOPIOL or BHS), KKLP applies to anions as well as to cations, and is an integral part of Hartree-Fock approximation.

Chapter III

THE PROGRAM, ICECAP

3.1 INTRODUCTION

ICECAP is a self-consistent lattice relaxation and electronic structure program package for performing calculations of the electronic structure of point-defects in ionic crystals. It is based on a physical model which has a quantum-mechanical defect cluster embedded in a shell model lattice, solved variationally by energy minimisation with respect to cluster parameters and lattice configurations maintaining finite-order multipole consistency between the cluster and the lattice. This model is essentially the same as described by Vail et al.[VHHS 82] and is discussed in section(3.2). We briefly give an outline of the program-package ICECAP in section(3.3). For a detailed discussion, we refer to a report[HHK+ 84] describing the program organisation, the required input data for a given problem and the procedure for the execution of the program. We note here that ICECAP is adapted to IBM/Amdahl, VAX/FPS and CRAY systems.

3.2 METHOD

We define the defect cluster as any excess electrons, plus those ions that are significantly perturbed by the defect, including both perturbations of their electronic structure and displacements of their nuclei. The electrons of the cluster are treated quantum-mechanically in the UHF-SCF approximation. The surrounding infinite lattice is a perturbed shell model crystal in which the ions are represented as dipole polarizable point charge combinations.

The coordinates of nuclei and of ions in the cluster are collectively denoted $\underline{Rc}$, referred to as the cluster configuration. Coordinates of the surrounding shell model lattice(core and shell positions of all the ions in the surrounding lattice) are collectively denoted $\underline{R}$, referred to as the lattice configuration. Electronic coordinates (positions and spins) of the cluster are denoted collectively by $\underline{r}$. The many-electron wavefunction for the cluster is denoted by $\Psi(\underline{r}\ \underline{Rc},\alpha)$, indicating parameteric dependence on the cluster configuration $\underline{Rc}$ and a set of electronic variational parameter $\underline{\alpha}$.

We write the total defect crystal energy E as

$$E(\underline{R},\underline{Rc},\alpha) = Ec(\underline{Rc},\underline{\alpha}) + Ec_{\ell}(\underline{R},\underline{Rc},\alpha) + E_{\ell}(\underline{R},\underline{Rc}) \qquad (3.2.1)$$

where Ec is the expectation value of the energy of the cluster in a given quantum state(ψ), including electronic kinetic energy and interaction among all nuclei, ions and electrons in the cluster; E_ℓ is the energy of the classical lattice($\underline{R}$) and Ec_ℓ is the cluster-lattice interaction.

Assuming that the strong localisation of ions in an ionic crystal provides a boundary condition for which the quantum-mechanical cluster does not significantly overlap the surrounding classical lattice, we divide the cluster-lattice interaction into classical Coulomb interaction and short-range interaction, which simulates quantum-mechanical effects. Thus, we write,

$$Ec_\ell(\underline{R},\underline{Rc},\underline{\alpha}) = V(\underline{R},\underline{Rc},\underline{\alpha}) + Es(\underline{R},\underline{Rc}) \qquad (3.2.2)$$

where V and Es are the cluster-lattice Coulomb and short-range interactions respectively. The short-range cluster-lattice interaction is taken to be the same as the short-range ion-ion interaction of the surrounding lattice. The total defect crystal energy is then,

$$E(\underline{R},\underline{Rc},\underline{\alpha}) = Ec(\underline{Rc},\underline{\alpha}) + V(\underline{R},\underline{Rc},\underline{\alpha}) + E_\ell'(\underline{R},\underline{Rc}) \qquad (3.2.3)$$

where E_ℓ' represents the energy of the classical lattice, plus its short-range interaction with the cluster. The total energy E, is now minimised with respect to cluster parameters $\underline{Rc}$ and $\underline{\alpha}$, and simultaneously with respect to lattice configuration $\underline{R}$, that is,

$$\left(\delta E / \delta \alpha \right)\Big|_{\underline{R}_c, \underline{R}} = \{ \delta (Ec+V) / \delta \underline{\alpha} \} = 0 \qquad (3.2.4)$$

$$\left(\delta E / \delta \underline{R} \right)\Big|_{\underline{R}_c, \underline{R}} = \{ \delta (V+E_{\ell}') / \delta \underline{R} \} = 0 \qquad (3.2.5)$$

$$\left(\delta E / \delta \underline{Rc} \right) = 0 \qquad (3.2.6)$$

yielding a variational estimate of cluster($\underline{Rc}$), electronic($\underline{\alpha}$), and lattice($\underline{R}$) configurations and of total defect crystal energy(E) and electronic wavefunction(Ψ).

To solve equation(3.2.6) subject to equations(3.2.4) and (3.2.5) simultaneously, we replace V by V' which is the Coulomb interaction between the lattice and cluster simulators (a small set of point charges simulating the cluster). The equation(3.2.5) now becomes

$$\{ \delta (V'+E_{\ell}') / \delta \underline{R} \}\Big|_{\underline{R}_c} = 0 \qquad (3.2.7)$$

This step is necessary to simplify the problem of solving the equation(3.2.6), since equation(3.2.5) with equation(3.2.4) requires variation of $V(\underline{R}, \underline{Rc}, \underline{\alpha})$ with respect to many ionic coordinates $\underline{R}$ for each configuration of which the Coulomb interaction V with the quantum-mechanical cluster must be evaluated. This is, however, prohibitively expensive in computer time.

The cluster simulators are chosen such that their charges and positions allow them collectively to have the same low-order electric multipole moments as the cluster. This can be achieved as follows :

(i) We begin with a fixed cluster configuration($\underline{Rc}$) and an associated set of cluster simulators, and solve equation(3.2.7) to obtain a first estimate for $\underline{R}$, the lattice configuration.

(ii) In the presence of this lattice configuration, we evaluate the multipole moments, collectively denoted by M, up to some finite order n for the quantum-mechanical cluster($\underline{Rc}$,$\underline{\alpha}$).

(iii) We now readjust the cluster-simulator charges and positions, keeping $\underline{Rc}$ fixed until their collectively multipole moments, denoted by M', agree with the set M up to order n.

(iv) We iterate these steps until the cluster and cluster simulator multipole moments, M and M' respectively, are consistent to order n.

At this stage, we have a lattice configuration($\underline{R}$) in equilibrium with a set of cluster simulators that have the same multipole moments, up to order n, as does the cluster whose electronic configuration($\underline{\alpha}$) is in equilibrium with $\underline{R}$, all for a given cluster configuration $\underline{Rc}$. We say that that $\underline{R}$ and $\underline{\alpha}$ are consistent to multipole order n. Finally, we

vary $\underline{Rc}$, maintaining n-th order consistency, to minimise E, satisfying equation(3.2.6). This solution with n-th order multipole consistency can be assessed from the multipole expansion of V, the cluster-lattice Coulomb interaction.

Suppose that the lattice consists of point charges Q at positions $\underline{R}$. Then, we write

$$V(\underline{R},\underline{Rc},\alpha) = \sum_j Q_j \int d^3r \quad \rho / |\underline{r}-\underline{R}_j| \quad . \tag{3.2.8}$$

where $\rho(\underline{r}, \underline{Rc},\alpha)$ is the charge density of cluster configuration $\underline{Rc}$. A similar formula applies for V', where ρ refers to the charge density of the point-charge cluster simulators.

Since V represents the interaction of the cluster with all the ions outside the cluster, we have $|\underline{R}_j| > |\underline{r}|$ in equation (3.2.8) and, for this case, V can therefore be expressed as a multipole expansion about the origin in the cluster, i.e.,

$$V(\underline{R},\underline{Rc},\alpha) = \sum_j Q_j \sum_{n=0}^{\infty} M^{(n)} / |\underline{R}_j|^{(n+1)} \tag{3.2.9}$$

where

$$M^{(n)}(\underline{Rc},j) = \ell_{\lambda_1}(j) \ldots \ell_{\lambda_n}(j)\, M_{\lambda_1 \ldots \lambda_n}(\underline{Rc}) \tag{3.2.10}$$

with Einstein summation conventions on λ_k (=1,2,3) and k=1,2,..,n. Here, ℓ (j) are cartesian components of the unit vector, that is,

$$(\ell_1(j),\ell_2(j),\ell_3(j)) = \underline{R}_j/|\underline{R}_j| \qquad (3.2.11)$$

In equation (3.2.10), $M^{(n)}$ are the n-th order multipole moments of the cluster's charge distribution(ρ).

The three lowest-order multipole moments are

(i) the total charge,

$$M^{(0)} = \int d^3r\ \rho$$

(ii) the dipole moment,

$$M_\alpha^{(1)} = \int d^3r\ r_\alpha\ \rho$$

(iii) the quadrupole moment,

$$M_{\alpha\beta}^{(2)} = \int d^3r\ \ (3\ r_\alpha r_\beta - r^2\delta_{\alpha\beta})\ \rho$$

where r_α are the cartesian coordinates of the position vector $\underline{r}$.

Thus, if V' in equation (3.2.7) agrees with V in equations (3.2.5) and (3.2.8) to order n, then the error involves only contributions to the energy of order $(\underline{R}_j)^{-(n+2)}$.

3.3 THE PROGRAM

ICECAP defines several classes of entities in order to ensure that each class must have their coordinates varied only in the appropriate portion of the program and that the interaction between any two entities must be taken into account exactly once, that is, neither omitted nor double counted. The classes of entities defined are :

(a) Ions that will be replaced by bare nuclei plus electrons,

(b) Ions that will be replaced by core pseudopotentials plus valence electrons,

(c) Ions that will be replaced by complete-ion pseudopotentials or Kunz-Klein localisation potentials(KKLP),

(d) Shell model ions that will be explicitly moved about in minimising the total defect crystal energy,

(e) Point charges simulating excess electrons in the cluster (electronic simulators),

(f) Point charges simulating multipole corrections(multipole simulators),

(g) Shell model ions of the surrounding lattice.

Classes (a) through (c) define the quantum-mechanical (UHF-SCF) region, whereas classes (a) through (f) define the cluster. The embedding lattice region is defined by entities in class (g). Class (e) is chosen initially to simulate the deviations of the charge distribution of the UHF-SCF region from the point-charge (shell model) distribution of classes (a) to (d). After a given run of the calculation, ICECAP may introduce point-charges of class (f) by the multipole consistency routines to correct low-order multipole moments of the cluster region simulated in HADES. Point-charges of classes (e) and (f) exert only Coulomb forces, but do not interact among themselves, nor with ions of classes (a) to (d), except that point-charges of class (e) do interact with shells of ions in classes (b) to (d). Thus dipole polarization of ions in the cluster, not

otherwise provided by quantum-mechanical electrons is included.

The program-package, ICECAP consists of a master driver program which generates data files for several programs. This method of organisation minimises the number of changes which have to be made to large pre-existing codes, namely HADES and UHF^{+}. The programs which are under the control of the driver are CRYDFN(the HADES symmetry analysis routine), RUN(the HADES lattice relaxation routine), UHF^{+}(LABELS, POLYIN and UHFABK routines), PROPS(molecular properties evaluation routine), MPFIT(multipole consistency routine) and TOTMIN(total energy minimisation routine). The bulk of computing is not concentrated in very few kernels, but is rather scattered over various program sections. Also, IO(input/output) operations associated with the two-electron integrals requires a lot of disk usage. For example, a calculation of 18 atoms(180 electrons) with 97 basis functions requires about 3000T disk space for the LABEL file, containing the list of integrals. It is to be noted here that some of my thesis work was in development of ICECAP, particularly in writing the MPFIT routine.

The MPFIT routine provides multipole consistency between the embedded cluster and the surrounding lattice up to octopole order. First, the multipole moments M and M' due to the UHF cluster and point-charge cluster simuators from

HADES are generated respectively. Then the MPFIT routine introduces point-charges,referred to as multipole simulators. They are determined from the difference between the multipole moments, M and M', by solving the system of non-linear equations from a given initial approximation. The solution provides the corresponding multipole strengths and direction cosines of displacements from which the charges and positions of multipole simulators are returned to the calling routine.

In its original form, the program ICECAP requires core space of 7.5 Mbytes, which is in excess to that available, 5 Mbytes, in the University of Manitoba (Amdahl 5870) computer system. This diffculty has been overcome by rearranging the program into an overlay structure, so that only those segments needed in executing a given calculation step are in core for the duration of that step. The overlay structure is along the lines suggested by Harker[Hark] and reduces the core requirement substantially from 7.5 Mbytes to 4.5 Mbytes, a 40% reduction.

The operating procedure of ICECAP, illustrated in Figure 3.1, is executed under the direction of the driver and can be summarised as follows :

(1) For a given cluster configuration, the excess electrons and the cluster ions are simulated by fixed point charges, from which HADES determines the polarized, distorted lattice

Figure 3.1 : Schematic diagram describing the operating procedure of the program package, ICECAP.

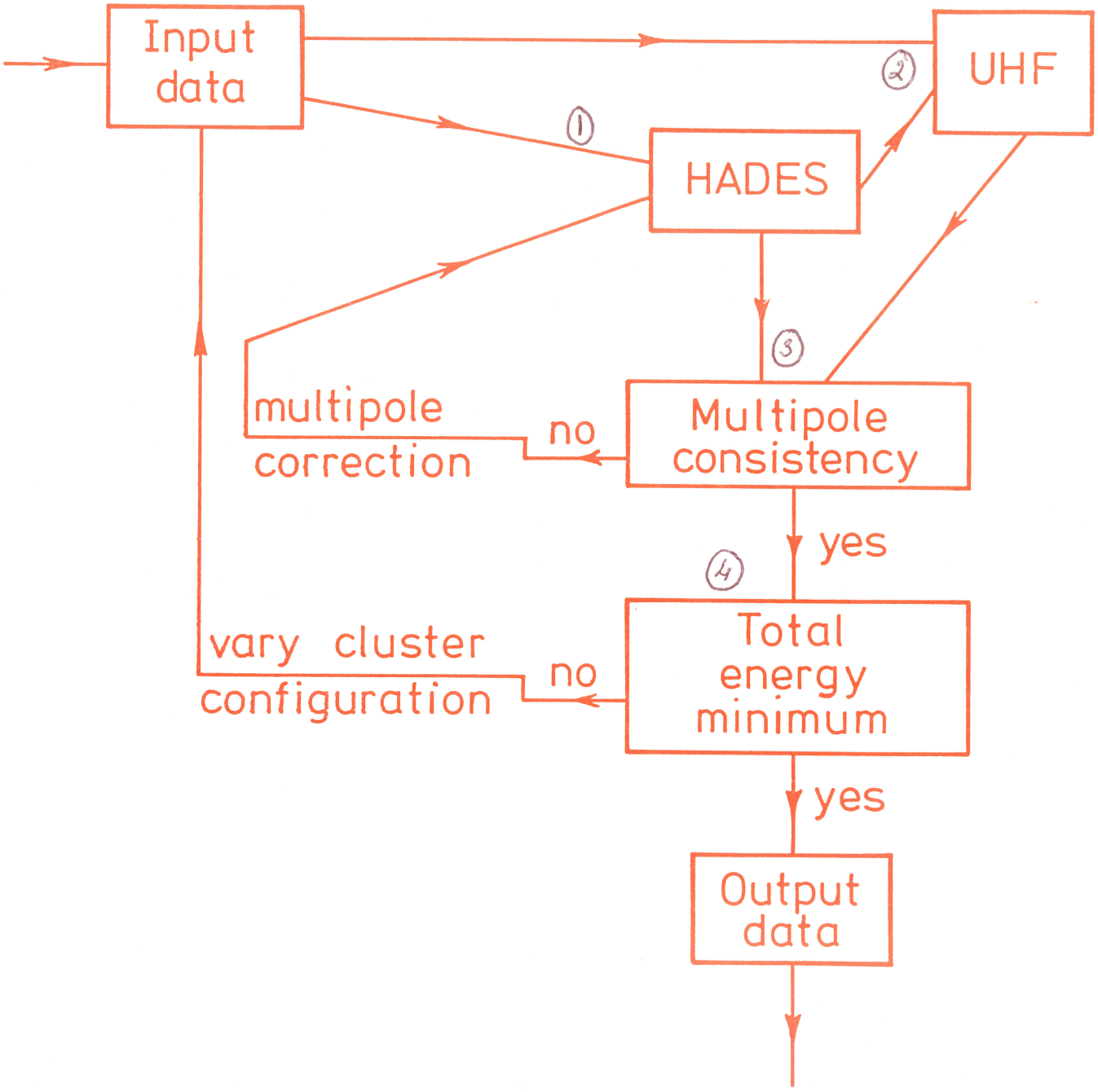
Input data
UHF
HADES
multipole correction
no
Multipole consistency
yes
vary cluster configuration
no
Total energy minimum
yes
Output data
1
2
3
4

configuration and the total energy of the point-charge simulated lattice(Eh).

We may now write,

$$E_{\ell}' = Eh - Ec' - Es' - \Delta V' \qquad (3.3.1)$$

where, E_{ℓ}' is the same as in equation(3.1.7), the interaction energy among all ions outside the cluster plus short-range cluster-lattice interaction;

Es' is the short-range plus shell-core interaction energy of any shell model ions that are included in the cluster-simulator set;

Ec' is the Coulomb interaction of the cluster simulators among themselves plus their Coulomb interaction with regions I and IIa(of HADES); and

$\Delta V'$ is the Coulomb interaction of the cluster simulators with region IIb(of HADES).

Here, it is assumed that shell-shell and shell-core interactions are simulated by electron-electron and electron-pseudopotential/KKLP interactions, except that in the case of a complete-ion psudopotential, where the shell-core interaction is not included. Both the terms Ec' and Es' are therefore subtracted from the energy Eh. Furthermore, shells in the cluster region(classes (a) to (d)) are free to respond to all point-charges in HADES except class(f), the multipole simulators.

(2) Shell model ions of the lattice, along with the cluster ions(i.e. nuclei/pseudopotentials/KKLP ions) of a fixed cluster configuration are now applied as a background potential for a UHF-SCF calculation. The total cluster energy(Ea) is evaluated by the UHF program package.

We may then write :

$$(Ec + V) = Ea + Eo + Ed + \Delta V \qquad (3.3.2)$$

where, Ec and V are defined as for equation(3.3.1), and ΔV is the Coulomb interaction of the cluster with region IIb, which is not evaluated. For nuclei, pseudopotentials or KKLP ions, i.e. for classes (a) to (c), the energy Ea includes their Coulombic interaction among themselves and with classes (d) and (g). The energy Eo represents a correction term for the energy of the dipoles simulating the polarization of ions associated with complete-ion pseudopotentials or Kunz-Klein localised potentials. It is assumed here that a dipole, including shell-core interaction can be carried over from a HADES shell model ion to a UHF complete-ion pseudopotential or a KKLP ion. Furthermore, HADES shell-shell interactions between classes (c) and (d) are assumed to be represented by their UHF short-range interactions.

The total defect crystal energy E (3.2.3) is then given by

$$E = (Eh-Ec'-Es') + (Ea+Eo+Ed) \qquad (3.3.3)$$

from (3.3.1) and (3.3.2), assuming that the term ($\Delta V-\Delta V'$) is negligible. This energy is evaluated at each iteration in working towards multipole consistency and overall energy minimisation.

(3) Ideally, the the cluster simulators should have all their multipole moments identical to those of UHF-SCF cluster. ICECAP, however, matches only a finite set of low-order multipole moments. This is accomplished by comparing, in the multipole consistency routine, a given set of low-order multipole moments(presently up to and including octopole) for classes (a) to (c) as calculated from the HADES and UHF$^+$ programs. If consistency is not found, additional point-charge simulators, called multipole simulators(class (f)), are introduced. Their positions and charges are evaluated by the multipole consistency routine such that when added into HADES they produce agreement to a required accuracy between HADES and UHF$^+$ multipole moments. ICECAP now iterate the HADES/UHF$^+$ sequence to consistency.

(4) Finally, the driver minimises the total energy E, as given by the equation(3.3.3) with respect to the cluster configuration(classes (a) to (d)), maintaining multipole consistency between the cluster and the embedding lattice.

ICECAP is based on HADES and UHF+ program packages, both of which have been extensively tested, refined and applied to point-defect calculations in ionic crystals. Consequently, any point-defect configuration in any ionic crystal host lattice geometry can be analysed, provided shell model parameters are available. Atomic orbital sets may include s, p, d and f types. Either norm-conserving BHS or Philips-Kleinman TOPIOL pseudopotentials can be used, and Kunz-Klein orthogonalisation procedure can be applied at the cluster boundary. Octopole consistency is presently available. Correlation correction can be included in the total energy, using a many body perturbation theory(MBPT) developed by Kunz[Kunz 83w]. The whole set of input data necessary for a calculation of the ground state of the F^+ center in magnesium oxide with the appropriate JCL for our computer system (Amdahl 5870) is given in the appendix.

The ultimate test of the physical model on which ICECAP is based can be made through comparisons with experimentally observed properties. For example, optical absorption and luminescence measure splittings between energy levels, whereas spin resonance can measure the square modulus of the wavefunction at a particular site. ICECAP does calculation of energy levels and wavefunctions and the subsquent calculation evaluates experimentally measurable quantities. If the results of such a comparison are favourable, the model acquires predictive credibility and can then be used

to study point-defects for which experimental data is either lacking or scarce. Hence, with this attitude, we now apply ICECAP to study the electronic structure of the point-defect, F^+ center in magnesium oxide and present the results in the following chapter.

Chapter IV

RESULTS AND DISCUSSIONS

The principal applications of ICECAP will be to point-defect properties, particularly those for which deviations from perfect lattice electronic structure are crucial. We have chosen to examine properties of a well-documented color center, the F^+ center in magnesium oxide which involves not only perturbations of ionic electronic structures, but also electronic states associated with vacancies. These color center states may be considerably more diffuse than ionic states, and through their optical transitions and hyperfine interactions with neighboring nuclei provide a sensitive test of the accuracy with which distortion and polarisation of the surrounding lattice and the electronic states are being treated.

Preliminary calculations modelling the absorption and emission process of the F^+ center will be presented first, followed by the detailed investigation of the ground and unrelaxed excited states of the F^+ center in magnesium oxide.

4.1 F^+ CENTER

An electron trapped in an anion vacancy is called an F center in alkali halides whereas an analogous center in alkaline-earth oxides, the divalent cousins of alkali halides, is called an F^+ center. Its structure has been verified by the ENDOR experiment[UC 67] which maps the density of the electron trapped in the vacancy through its hyperfine interaction with the nuclear moments of the near-neighbor lattice ions.

The F^+ center has a number of electronic states and the optical absorption produces a transition of the trapped electron from the ground state to the first excited state. We note here that it is analogous to a one-electron atom, He^+ and we may therefore label its electronic states as 1s, 2s, 2p and so on. The first allowed optical transition is then between the 1s and 2p states. Since such a transition takes place on a time scale short in comparison to lattice vibrations, it will occur while the lattice atoms remain essentially at some fixed configuration. This is the Franck-Condon principle.

In the excited 2p state, the charge distribution has changed, and the interaction of the electron with those on neighboring ions(which are now relaxed to new lattice configurations) is different. Thus, the electronic energy in the relaxed excited state(2p*) has changed. Now, from

this state, the luminescence transition(2p* - 1s*) may occur at a fixed lattice configuration. The quanta of energy involved in optical absorption and luminescence transitions are therefore different and this energy difference is referred to as the Stokes shift.

The optical properties of F^+ center in the magnesium oxide are well-documented experimentally[Hend 80]. The F^+ absorption band is reported to be at 4.95 eV with a corresponding emission band at 3.13 eV, suggesting a large Stokes shift.

Magnesium oxide(MgO), the host lattice of the F^+ center in the present work, calls for a brief comment here. It belongs to the family of alkaline-earth oxides and is strongly ionic in character; the anions and cations having the rare-gas electronic configurations. It has an NaCl structure, with a lattice parameter of 4.2112 Å (i.e. near-neighbor distance(a)=2.1056 Å). There are two atoms per unit cell in which anions and cations form two interpenetrating face-centered cubic sublattices. Thus, anions and cations are arranged on alternate cube corners along the <100> directions, (~~and the «111» planes are alternatively composed entirely directions,~~) and the {111} planes are alternatively composed entirely of anions or cations. Several band structure calculations have been carried out, and these are in general qualitative agreement

as to the broad features of the valence and conduction bands[CDPR 86 and references therein].

4.2 THE MODEL

The program package, ICECAP, facilitates the computing of defect properties in ionic materials systematically and routinely in a standardized model. In this model, the embedded (quantum-mechanical) cluster consists of an excess electron, that is associated with an oxygen vacancy, plus six nearest-neighbor magnesium(Mg^{2+}) ions(Figure 4.1). These Mg^{2+} ions are represented by shell model (SM), pseudopotentials (TOPIOL/BHS), Kunz-Klein localised potential (KKLP) and gaussians centered on ionic sites, referred to as Hartree-Fock ions, in a series of calculations, presented here. The surrounding lattice is treated in the shell model.

Shell model parameters for MgO crystal are taken from the work of Sangster and Stoneham[SS 81], with Mg^{2+}ions unpolarisable and involving only nearest-neighbor short-range interactions but with O^{2-} ions polarisable and including second-neighbor short-range interactions as well. These parameters which are given in Table 4.1, reproduce the perfect lattice properties of MgO crystal reasonably well(Table 4.2).

Figure 4.1 : F^+ center in MgO crystal.
Solid line indicates (quantum-mechanical) defect cluster region. Ions with dashed line are included in the cluster in the later part of the study.

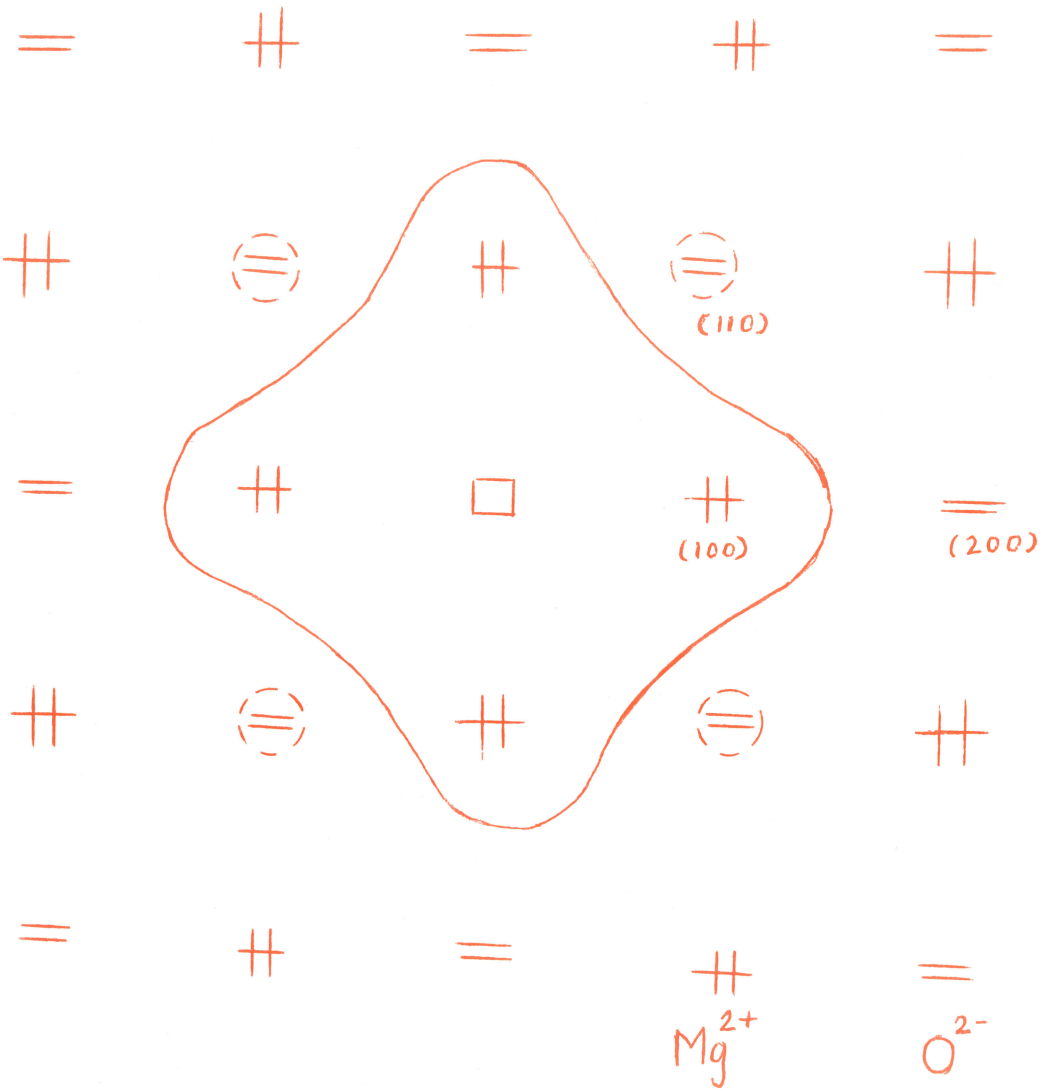
(110)
(100)
(200)
Mg2+
O2-

TABLE 4.1

Parameters of the Shell-model and Short-range Potential ($V = A \exp(-r/\rho) - cr^{-6}$)

Shell-model parameters	Shell Charge (e)	Spring Constant (eV A^{-2})
Mg^{2+}	unpolarisable	
O^{2-}	2.81	46.125

Potential	A (eV)	ρ (A)	C (eV A^6)
$Mg^{2+} - O^{2-}$	1275.2	0.3012	0.0
$O^{2-} - O^{2-}$	22764.3	0.1490	20.37
$Mg^{2+} - Mg^{2+}$	-	-	-

TABLE 4.2

Calculated and Observed Perfect Lattice Properties of Magnesium Oxide.

Properties	Calculated	Observed
lattice spacing (A) (near-neighbor distance)	2.106	2.106
dielectric constants		
ϵ_c	9.77	9.86
ϵ_∞	2.96	2.96
lattice energy (eV)	-40.9	-40.4
elastic constants (10^{12} dynes/cm^2)		
C11	3.71	2.89
C12	1.57	0.88
C44	1.57	1.55

4.3 PRELIMINARY CALCULATIONS

Our preliminary calculations involve the one electron F^+ center, either placed alone in a shell model lattice or with nearest-neighbor cations represented by pseudopotentials (TOPIOL/BHS), Kunz-Klein localised potential(KKLP) or Hartree-Fock ions.

For the one electron F^+ center, s- and p-type basis functions(Basis FC) are used for ground and excited states of the F^+ center respectively. Basis FC consists of 9 gaussian primitives. Table 4.3 lists the actual values of α along with their corresponding range, defined by $(2\ \alpha)^{-1/2}$. This range is the distance at which the charge density of an s-type gaussian is e^{-1} times its maximum, and of a p-type gaussian is maximum. For Mg^{2+} ions (atomic number:12) which are represented as Hartree-Fock(HF) ions, we use Huzinaga's smallest optimal minimal basis set[Huzi 84], referred to as Basis MGA. It is based on free-atom contractions(3,3/3) for 1s, 2s and 2p cation states. We note here that the numerical values in the contration symbol represent the number of primitive Gaussians contracted to single atomic orbitals. Basis MGA is listed in Table 4.3 which also includes an oxygen basis set(Basis OXA) used in the later part of this work.

For each electronic optical transition energy, denoted Ea for absorption and Ee for emission, two calculations are

TABLE 4.3

Basis Sets Associated with Vacancy, Mg^{2+} ions and O^{2-} ions.

(i) Vacancy :

Basis FC

type	exponent	range
s/p	0.974	0.18a
	0.244	0.36a
	0.108	0.54a
	0.061	0.72a
	0.027	1.08a
	0.015	1.44a
	0.010	1.80a
	0.007	2.10a
	0.004	2.80a

where a = 3.979 bohr, the nearest-neighbor distance in MgO.

(ii) O^{2-}-Ions :

	Basis OXA (3,3/3)	
type	exponent	coefficient
| 1s >	281.86658	0.0690599
	42.41600	0.3931595
	9.09562	0.6656691
| 2s >	11.46603	-0.0808199
	0.88786	0.5820895
	0.27880	0.4971596
| 2p >	8.04724	0.1242709
	1.66842	0.4765935
	0.37251	0.6130445

(iii) Mg^{2+}-Ions :

type	exponent	Basis MGA (3,3/3) coefficient	Basis MGR (3,3,1/3,1) coefficient
| 1s >	650.64367	0.0680297	0.033942
	98.37078	0.3907384	0.188603
	21.32249	0.6672673	0.275350
| 2s >	27.97738	-0.0867195	-0.066825
	2.32652	0.5856969	0.341160
	0.81808	0.4864974	0.290599
| s' >	7.47	-	1.0
| 2p >			axial-
	23.21663	0.1214603	0.049178
	5.00222	0.4792914	0.195580
	1.20465	0.5989417	0.242770
			non-axial
			0.044945
			0.178684
			0.221938
| 2p' >	0.1973	-	1.0

required; one for the initial state in which the lattice is relaxed to equilibrium with the cluster, and the other for the final state in which the ionic positions and polarisations are held fixed in the initial state configurations. Thus we have four states, namely, ground state(GS), unrelaxed excited state(UNRES), relaxed excited state(RES) and unrelaxed ground state(UNRGS). The lattice configuration is the same for both states of a transition. For absorption, they are determined by the ground state and through symmetry are equal (d) for all six nearest-neighbors. For emission, they are determined by the relaxed excited state, which is assumed to involve a p-type state oriented along the z-axis. The two axial neighbors are therefore displaced to (dz) whereas the other four neighbors are displaced equally in the x-y plane, radially to (dx). The mean radial distance(RMS), $\langle r^2 \rangle^{1/2}$, represents the extent of the localisation of the electronic density that is associated with F^+ center electron in a given state and is different for each state. We present the results in Table 4.4. The calculated transition energies are compared with corresponding experimental values in Table 4.5.

Referring to Tables 4.4 and 4.5, we note that a single quantum-mechanical electron(with Basis FC) in a shell model lattice reproduces experimental absorption energy very well, and emission energy roughly, associated with reasonably well-localised wavefunctions in all four states. However,

TABLE 4.4

Results of Preliminary Calculations.

(Basis FC - Vacancy)

(a) SM-NN

	GS	UNRES	RES	UNRGS
energy (eV)	18.33	23.18	21.93	19.12
d (dx, dz)	1.03a		(1.07a, 0.98a)	
RMS	0.74a	0.93a	0.91a	0.76a

(b) KKLP-NN

energy (eV)	19.38	24.53	22.95	20.50
d (dx, dz)	1.03a		(1.10a, 0.92a)	
RMS	0.68a	1.51a	1.63a	0.73a

(c) TOPIOL-NN

energy (eV)	25.28	26.12	25.53	(25.83)
d (dx, dz)	1.09a		(1.10a, 1.0a)	
RMS	1.77a	2.69a	2.34a	2.41a

continued...

(d) BHS - NN

	GS	UNRES	RES	UNRGS
energy (eV)	21.07	26.31	25.46	23.63
d (dx, dz)	1.05a		(1.10a, 1.0a)	
RMS	0.63a	2.14a	2.21a	0.73a

(e) HF - NN

(Basis MGA)				
energy (eV)	-32256.90	-32251.71	-32253.38	-32254.45
d (dx, dz)	1.04a		(1.10a, 1.0a)	
RMS	0.64a	2.17a	2.23a	0.73a

TABLE 4.5

Calculated Absorption and Emission Energies of the F^+-center.

nearest-neighbors	Absorption Energy (eV)	Emission Energy (eV)
Shell-Model	4.85	2.81
KKLP	5.15	2.45
TOPIOL	0.84	(-0.30)
BHS	5.24	1.83
HF (Basis MGA)	5.19	1.07

note : F^+-center absorption and emission energies are reported to be 4.95 eV and 3.18 eV respectively[Hend 80].

when the ion-size effects are introduced, the picture changes. With KKLP, BHS and Hartree-Fock nearest-neighbors, the ground state remains well-localised, with slight lattice distortion (~5%). Similarly, in the unrelaxed excited state we expect to find the wavefunction localised inside the vacancy. But, on the contrary, the wavefunction does not remain localised, and spills well beyond the nearest-neighbor distance(RMS > 1.5a). In other words, the p-type function has significant amplitude beyond the nearest-neighbors. The agreement with the experimental absorption energy thus becomes poorer.

The relaxed excited state(RES) wavefunction is similarly diffuse, but the calculated emission energies are very wrong(Table 4.5). We note how quadrupole consistency associates an oblate nearest-neighbor configuration with the prolate p-type state RES wavefunction oriented along the z-axis, in all cases(Table 4.4). However, with TOPIOL, the calculated results are completely unphysical, with extremely small absorption energy. The s-type UNRGS state turns out to be above the p-type RES state, resulting in a negative emission energy. It appears that the ion-size effect of TOPIOL is greater than that of either KKLP/BHS or Hartree-Fock, judging by wavefunction diffuseness(Table 4.4).

Thus, the results suggest that TOPIOL pseudopotentials do not prove to be appropriate model elemets for representing

the electronic structure of Mg^{2+}ions in the present calculations. Furthermore, the ion-size effect of anions on the z-axis in UNRES and RES p-type states seems to be important as p-type functions, oriented along the z-axis spill beyond the nearest-neighbor. The anions(oxygen ions) are the second nearest-neighbors and are represented by shell model point-charge ions in these calculations.

Similar results have been obtained by us with a different vacancy-centered basis function (consisting of 5 gaussian primitives) in an earlier investigation[VP 86].

We now associate Kunz-Klein localised potential(KKLP) with the ions beyond the nearest-neighbor ions of the vacancy to provide the ion-size effect, since neither TOPIOL nor BHS pseudopotentials are availble for anions. The results are given in Table 4.6. Here, we find that the introduction of KKLP localises the UNRES wavefunction (RMS $\sim$ a). But the calculated absorption energy turns out to be totally wrong.

In examining the Mulliken population over vacancy-centered basis function(Basis FC), we notice that some of the primitives have sizeable negative Mulliken population in both the ground and unrelaxed excited states (Table 4.7). For UNRES state, the dominant components correspond to the primitives of ranges 1.08a, 1.44a and 1.80a respectively; the first two have opposite signs, thereby leaving the third

TABLE 4.6

F^+-center : ion-size effect

(Basis FC - vacancy)
(Basis MGA - Mg^{2+} ion)

2,3,4,5,6,7 nearest-neighbor ions of vacancy	Shell-Model ions	KKLP ions
Absorption Energy (eV)	5.19	7.65
(i) Ground State :		
energy (eV)	-32256.90	-32261.08
d	1.04a	1.01a
Mulliken Population - vacancy	1.0163	1.0102
RMS	0.64a	0.58a
(ii) Unrelaxed Excited State :		
energy (eV)	-32251.71	-32253.43
Mulliken Population - vacancy	1.0218	1.0238
RMS	2.17a	1.03a

TABLE 4.7

Vacancy Basis Set : Mulliken Population

(Basis MGA - Mg^{2+}-ions)
(no KKLP ion-size effect)

BASIS FC (Vacancy)

exponent range (a)	Mulliken Population	
	GS	UNRES
0.18	0.0006	0.0007
0.36	-0.1828	-0.0478
0.54	1.9251	0.5848
0.72	-1.2521	-1.2060
1.08	1.0174	2.3687
1.44	-0.8818	-2.3398
1.80	0.5967	2.4440
2.10	-0.2252	-0.8505
2.80	0.0184	0.0677

one as a resultant whose range is well-beyond the nearest-neighbor distance. Thus, the delocalisation appears to be spurious and may be due to overlapping of primitives, forming the UNRES wavefunction. The calculations with KKLP ion-size effect have also shown negative Mulliken population associated with some of the primitives of the function, Basis FC.

Experience has shown that negative Mulliken populations for basis orbitals, arising as they do from predominance of overlap compared to direct contributions, should be taken as an indication of present or incipient linear-dependence failure of the calculation[VW]. Hence we go back and look closely into our model elements, namely vacancy-centered and Mg^{2+} basis functions in the defect cluster for ground and excited states of the F^{+} center.

4.4 GROUND STATE

For the ground state, we start with a single gaussian, centered at the vacancy and optimise its range in a defect cluster; a vacancy and six nearest-neighbor Mg^{2+} ions represented by Basis MGA. The optimum range of the s-type ground state wavefunction comes out to be 0.63a as shown in Figure 4.2.

We now look into the other model element, Mg^{2+} basis set(Basis MGA) and notice that it is constructed by

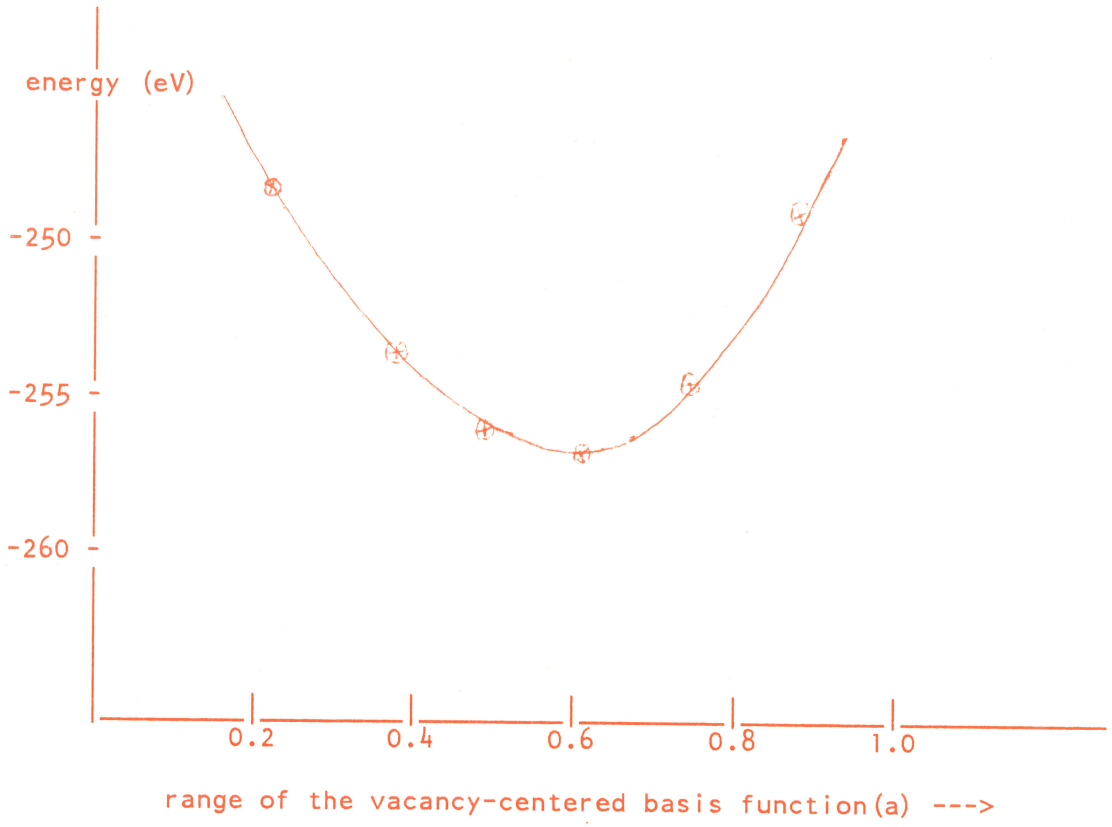

Figure 4.1 : Optimisation of the vacancy-centered basis function in the ground state (Mg^{2+} ion - Basis MGA).

optimisation of the Hartree-Fock energy of a free Mg atom. This choice places heavy emphasis on representing the core orbitals, as these orbitals contribute most of the total energy of an atom. If the atom is placed in a cluster environment, additional diffuse primitives may be needed to describe its (electronic density) distortion in the cluster environment. Furthermore, Basis MGA does not take account of core polarisation in an asymetric environment, provided by the vacancy to nearest-neighbor Mg^{2+}ions in our defect cluster. We therefore reoptimise Basis MGA in a realistic crystalline environment.

In basis-set optimisation, we de-contract the (free) atomic basis-set, re-contract them in the (relaxed) lattice containing the defect, and optimise the ranges of additional s- and p-type primitives at ionic sites.

The procedure consists of the following steps :

(i) First, we de-contract Basis MGA(3,3/3). Primitives are now allowed to vary independently in the UHF calculation increasing the number of basis functions from 31 to 91 in the defect cluster.

(ii) The self-consistent solution of the cluster, obtained from ICECAP calculation provides new contraction coefficients for the basis functions associated with 1s, 2s and 2p orbitals.

(iii) We now contract the 1s orbital only and repeat the calculation with decontracted 2s and 2p orbitals. From this calculation, we contract the 2s orbital.

(iv) Finally, the next calculation with contracted 1s and 2s orbitals gives the new contraction coefficients for 2p orbitals.

This reoptimised Mg^{2+} basis set, referred to as Basis MGR is given in Table 4.3 and is a contraction of (3,3/3). We notice that the contraction coefficients of axial p-type orbital (pointing towards the vacancy) are different from the other two non-axial p-type orbitals, reflecting the asymmetric environment for the nearest-neighbor Mg^{2+} ions in the defect cluster.

We now add primitives of both s- and p-type to Basis MGR to increase the flexibilty of the basis set. The most widely used quality criterion for the basis set has been the total energy test and is adapted in our work. Care has been taken to avoid the negative Mulliken population on the basis functions. Accordingly, s- and p-type primitives of ranges 0.065a and 0.4a repectively gives the minimum total energy for the defect cluster for the ground state(Figure 4.3, Table 4.8). We have included these primitives in Basis MGR for our subsquent calculations.

Referring to Figure 4.3, we notice that the addition of an (optimised) s-type primitive to Basis MGR lowers the total energy of the cluster by 60 eV. This primitive is of short-range ($\sim$0.065a), indicating the need of an additional s-type basis function for core states in the set, Basis MGR.

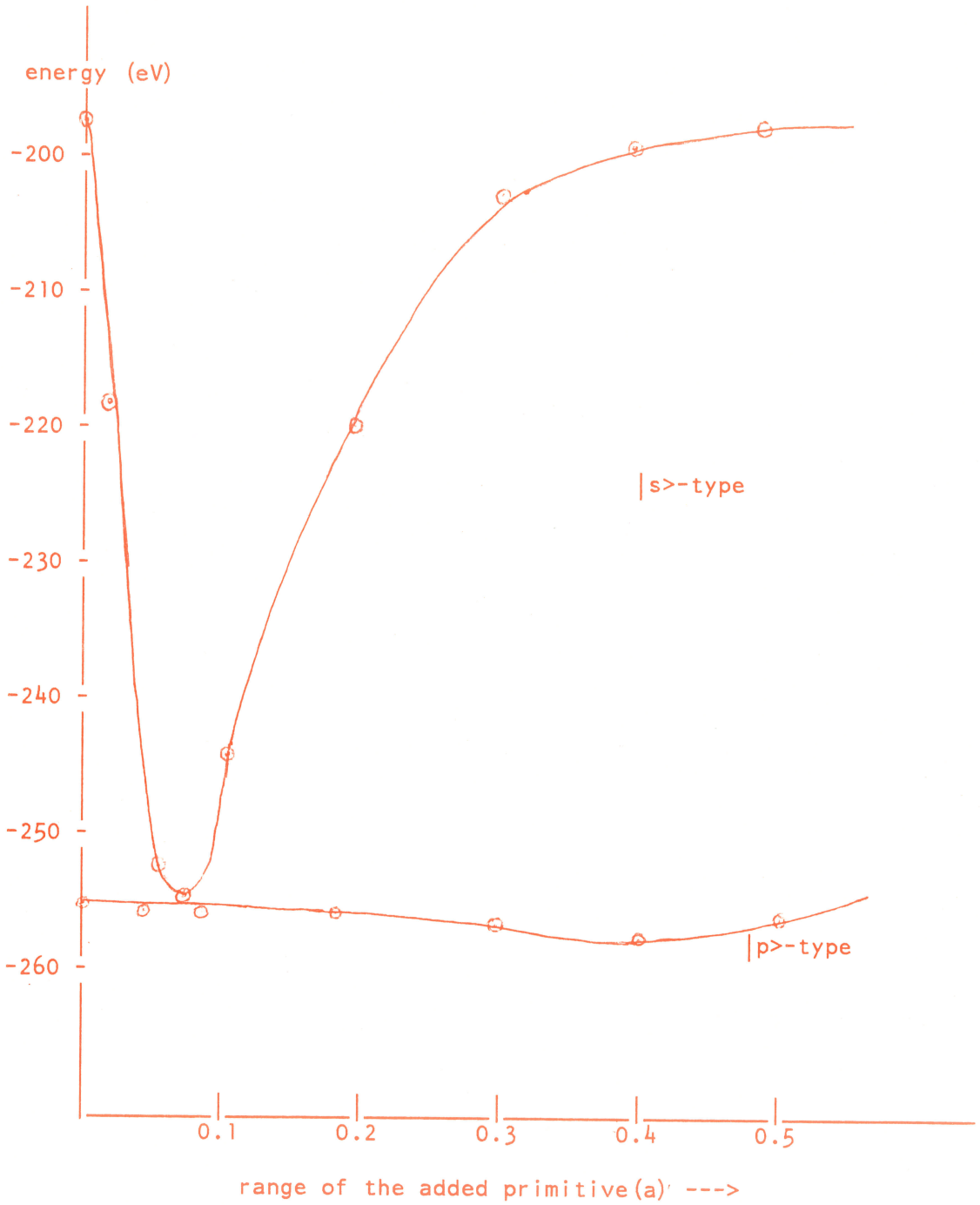

Figure 4.3 : Optimisation of the range of the added |s>- and |p>-type primitives to the Mg^{2+} basis set, Basis MGR.

TABLE 4.8

Ground State - Total Energy of the Cluster (F^+(e)-Mg6)

Mg^{2+} Basis Set	Energy (eV)
(a) Basis MGA (3,3/3)	-32256.06
- decontracted	-32271.13
- contracted	
1s	-32270.92
1s,2s	-32196.12
1s,2s,2p	-32195.66
(b) Basis MGR (3,3/3)	-32195.66
(c) (b) + s'	-32254.38
(d) (c) + p'	-32258.94

The additional (optimised) p-type primitive does not lower the total energy significantly and, in a limited sense, is expected to describe the distortion of the electronic density of Mg^{2+} ions in the cluster environment.

However, close examination of Table 4.8 reveals that the total energy of the defect cluster with reoptimised Mg^{2+} basis set(Basis MGR) is about 75 eV higher than that with the decontracted Mg^{2+} basis set. This increase in the total energy may be understood from the fact that the contraction coefficients of the basis functions associated with 1s and 2s orbitals are not obtained from pure 1s- and 2s-type eigenstates but instead are obtained from admixtures of 1s- and 2s-type eigenstates of the defect cluster.

We have therefore modified our procedure of basis-set optimisation and have obtained a new set of contraction coefficients for the basis functions in the following way :

(i) We do an ICECAP calculation with the decontracted basis set, Basis MGB. This set is a smallest optimal minimal basis set for Mg^{2+} ion(Table 4.9, Huzi 84). The self-consistent solution of the cluster then gives the new contraction coefficients for basis functions associated with 1s, 2s, and 2p orbitals.

(ii) We now read the coefficients for s-type functions(6 in the present case) from 1s- and ~~and~~ 2s-type eigenstates to form contractions for 1s and 2s orbitals.

TABLE 4.9

(a) Ground State : Total Energy of the Cluster (F^+(e)-Mg6)

	Energy (eV)
Basis MGB (3,3/3)	-32256.26
- decontracted	-32271.41
- contracted	
1s,2s	-32271.39
1s,2s,2p	-32271.39
Basis MGT (6,6/3)	-32271.39

(b) Mg^{2+} Basis Sets :

		Basis MGB (3,3/3)	Basis MGT (6,6/3)
type	exponent	coefficient	coefficient
| 1s >	654.890970	0.0675674	0.022845
	98.727577	0.3901195	0.127542
	21.335201	0.6683850	0.187178
	28.128657	-	0.032911
	2.295112	-	0.028823
	0.799752	-	-0.011074
| 2s >	654.890970	-	-0.010839
	98.727577	-	-0.066309
	21.335201	-	-0.114281
	28.128657	-0.0863368	-0.051193
	2.295112	0.5978077	0.379727
	0.799752	0.4746430	0.301423
| 2p >			axial-
	23.805108	0.1182192	0.033577
	5.116593	0.4748816	0.134761
	1.231392	0.6051010	0.172058
			non-axial
			0.058927
			0.236805
			0.300990

(iii) The next calculation with contracted 1s and 2s orbitals gives the new contraction coefficients for 2p orbitals.

The resulting Mg^{2+} basis set, referred to as Basis MGT, is a contraction of (6,6/3) and is given in Table 4.9. We notice here that the total energy of the cluster either with decontracted set or with reoptimised set remains the same, thereby indicating the improvement in our basis-set optimisation procedure.

Recently, Causa et al[CDPR 86] have reported a basis set for the Mg^{2+} ion, obtained from perfect lattice calculations of MgO crystal. It consists of the contraction (8,6/6) and is therefore expected to represent Mg^{2+} core states more adequately than the basis sets used here. However, we cannot reoptimise this set in the lattice containing the F^+ center as a decontracted set with 192 basis functions is too large to handle by our computer system.

The calculated ground state energy of the F^+ center with the different Mg^{2+} basis sets is given in Table 4.10. The optimised range of the vacancy-centered s-type basis function remains approximately the same, indicating a well-localised wavefunction for the ground state of the F^+ center in MgO crystal. Also, Mulliken population shows that there is no charge transfer either from Mg^{2+} ions to the vacancy or viceversa and approximately one electron is localised on the vacancy.

TABLE 4.10

Ground State : Mg^{2+} Basis Sets

(F^+(e)-Mg6 cluster)

Basis Set	MGR (3,3/3)	MGR + s'+ p' (3,3,1/3,1)	MGT (6,6/3)
Vacancy-centered Basis : range	0.60a	0.53a	0.50a
energy (eV)	-32195.74	-32258.94	-32271.73
d	1.04a	1.03a	1.03a
Mulliken Population (vacancy)	1.0054	0.9969	1.0054
RMS	0.72a	0.63a	0.60a

A final set of calculations has been done in order to assess the ion-size effect of second nearest-neighbor O^{2-} ions onto the ground state of the F^+ center. The defect cluster now contains 181 electron associated with a vacancy, six nearest-neighbor (100) Mg^{2+} ions and twelve second nearest-neighbor (110) O^{2-} ions. The third (111) and fourth (200) nearest-nighbors are associated with Kunz-Klein localising potentials.

For O^{2-} ions (atomic number:8) which are represented as Hartree-Fock ions, we use two basis sets, namely Basis OXA and Basis OXT. Basis OXA consists of the contraction (3,3/3) and is constructed by optimisation of the Hartree-Fock energy of a free oxygen atom[Huzi 84]. It is listed in Table 4.3. Basis OXT consists of the contraction (7,7/4) and is constructed by reoptimising the contraction coefficients in a perfect-lattice configuration of MgO crystal in the following way :

(i) In our O^{2-}-centered cluster, the six nearest-neighbor Mg^{2+} ions are associated with Basis MGC(4,3/4, Huzi 84) whereas the second nearest-neighbor (110) O^{2-} ions and the third nearest-neighbor (111) Mg^{2+} ions are associated with Kunz-Klein localising potential in the perfect-lattice configuration.

(ii) We now take the set Basis OXB(4,3/4, Huzi 84) and de-contract it. We then do an ICECAP calculation with the decontracted Basis OXB. The self-consistent solution of the

cluster provides the new contraction coefficients for basis functions associated with 1s, 2s, and 2p orbitals of O^{2-} ion.

(iii) We read the coefficients for s-type functions (7 in the present case) from 1s- and and 2s-type eigenstates to form contractions for 1s and 2s orbitals.

(iv) The next calculation with contracted 1s and 2s orbitals gives the new contraction coefficients for 2p orbitals.

The resulting O^{2-} basis set(Basis OXT) is given in Table 4.11. This table also includes the total energy of the perfect-lattice cluster with contracted, decontracted and reoptimised O^{2-} basis sets, showing a gain in the total energy of nearly 11 eV when we reoptimse the basis set.

The calculated ground state energy of the F^+ center in the cluster(Mg6O12) with different Mg^{2+}/O^{2-} basis sets is given in Table 4.12. Referring to this table, we notice that the ground state remains well-localised with slight lattice distortion, the (100) Mg^{2+} ions relaxing outward whereas (110) O^{2-} ions relax inward, by about 3% respectively. However, the calculation with Basis OXA (associated with O^{2-} ions in the cluster) shows that approximately 1.75 electron is localised on the vacancy due to a substantial charge transfer ($\sim$6%) from each of the twelve (110) O^{2-} ions to the vacancy. But when we associate an improved basis set, Basis OXT, with these O^{2-} ions, we

TABLE 4.11

(a) Total Energy of the Perfect-Lattice Cluster (Mg60)

		Energy (eV)
Mg^{2+} ions : Basis MGC (4,3/4)	Basis OXB (4,3/4)	-34435.49
	- decontracted	-34446.27
	- contracted	
	1s,2s	-34446.24
	1s,2s,2p	-34446.17
	Basis OXT (7,7/4)	-34446.17

(b) O^{2-} Basis Sets :

		Basis OXB (4,3/4)	Basis OXT (7,7/4)
type	exponent	coefficient	coefficient
| 1s >	821.83934	0.0188745	0.018970
	123.68182	0.1310931	0.133227
	27.66617	0.4577639	0.446412
	7.29957	0.5308957	0.471820
	10.60696	-	0.052033
	0.91764	-	0.043176
	0.28000	-	-0.013178
| 2s >	821.83934	-	-0.003963
	123.68182	-	-0.029757
	27.66617	-	-0.106846
	7.29957	-	-0.117476
	10.60696	-0.0885017	-0.074976
	0.91764	0.5838364	0.463203
	0.28000	0.4933946	0.637957
| 2p >	17.750370	0.0403941	0.034474
	3.86468	0.2236495	0.190821
	1.04772	0.5120981	0.370858
	0.28000	0.4443718	0.611384

TABLE 4.12

F^+-center : Ground State

(F^+(e)-Mg6012 cluster)

Vacancy (000) 1nn ions (100) 2nn ions (110) 3,4 nn ions	Basis FR Basis MGR Basis OXA KKLP	Basis FT Basis MGT Basis OXT KKLP
Vacancy- centered Basis : range	0.53a	0.50a
energy (eV)	-56271.08	-56535.08
d (100)	1.03a	1.03a
d (110)	1.00a	0.97a
RMS	0.87a	0.85a
Mulliken Population - vacancy	1.7512	1.0759
(100) Mg^{2+} ion	10.0000	9.9993
(110) O^{2-} ion	9.9409	9.9940

find very little charge transfer (0.6%) from O^{2-} ion to the vacancy. The vacancy now contains approximately one electron. Thus, Mulliken population analysis demonstrates the effect of 'reoptimisation' of the (free) atomic basis sets in these types of the calculation.

Theoretical prediction of the hyperfine constants has long been recognised as the most critical test of the defect model. The isotropic constant(a) is proportional to the electron spin-density at the nucleus and thereby furnishes an exact determination of the wavefunction amplitude in the ground state. We therefore calculate the isotropic constant to test our model elements for the ground state of the F^+ center in MgO crystal.

4.4.1 Ground State Isotropic Hyperfine Constant

The F^+-center electron which is an unpaired electron shows Zeeman splitting in the presence of a magnetic field. It also undergoes mutual magnetic interactions with neighboring nuclei which have non-zero nuclear spin, leading to further splittings. The latter phenomenon is referred to as hyperfine interaction. The theory of hyperfine interaction in color centers has been reviewed by Seidel and Wolf[SW 68]. Neglecting quadrupole effects, the spin Hamiltonian is written as :

$$H = g_e \mu_B \underline{B}.\underline{S} - \sum_\alpha g_N \mu_N \underline{B}.\underline{I}_\alpha + \sum_\alpha \underline{I}_\alpha.\underline{\underline{A}}.\underline{S} \qquad (4.4.1)$$

in which μ_B and μ_N are the electron and nuclear Bohr magnetons, g_e and g_N are the electron and nuclear g-factors, $\underset{\sim}{S}$ and $\underset{\sim}{I}$ are the electron and nuclear spin operators, $\underset{\sim}{B}$ is the applied magnetic field, and $\underset{\approx}{A}$ is the (second rank) hyperfine interaction tensor. The summation is over all the nuclei in the system. (For Mg^{25} nucleus, $g_N = -0.3419$ [SW 68])

The first two terms in (4.4.1) represent the electron-Zeeman and the nuclear-Zeeman effect respectively, and the last is the hyperfine structure term which splits each electronic level into 2I+1 hyperfine levels.

The hyperfine tensor, $\underset{\approx}{A}$ is generally written as the sum of two parts, a scalar 'a' and a traceless tensor '$\underset{\approx}{b}$'. The scalar is then referred to as the isotropic hyperfine interaction constant, and '$\underset{\approx}{b}$' describes the anistropic hyperfine structure. The magnitude of the hyperfine interaction is directly related to the extent of electronic overlap onto the neighboring nuclei. The isotropic part depends on the amplitude of the F^+-center electron at the nuclear site, and consquently relates to the radial extent of the wavefunction. The anistropic part involves a weighted average of the electron-spin density, and this turns out to be relatively sensitive to angular variations in the wavefunction.

Following Slichter[Slic 78], the isotropic constant can be written as :

$$a(\underline{R}_\nu) = \frac{8\pi}{3} g_e \mu_B g_N \mu_N S(\underline{R}_\nu) \qquad (4.4.2)$$

where $\underline{R}_\nu$ is the distance measured relative to the ν -th nucleus and $S(\underline{R}_\nu)$ is the spin density at the nucleus. Here, we use $\mu_B = 0.92731 \times 10^{-20}$ ergs/Gauss, $\mu_N = 0.50504 \times 10^{-23}$ ergs/Gauss, and S has units of cm^{-3} when 'a' is measured in ergs. Experimentalists quote 'a' in units of frequencies(MHz). The conversion factor into energy E expressed in ergs is $E(ergs) = 10^6 h(Mhz)$ where h is Planck's constant.

The Spin density S(R) for a N-body system is rigorously defined as :

$$S(\underline{R}) = 2 \int \Psi^*(x_1, \ldots x_N) \hat{S}z(\underline{R}) \Psi(x_1, \ldots x_N) \, dx_1 \ldots dx_N \qquad (4.4.3)$$

where, x_i represents the space-spin coordinates (r_i, σ_i), Ψ is the Slater determinant of one-electron orbitals $\phi_1(x_1) \ldots \phi(x_N)$ and $\hat{S}_Z(\underline{R})$ is the z-component of the total spin operator at point R given by :

$$\hat{S}_Z(R) = \sum_i \sigma_{Zi} \delta(\underline{r}_i - \underline{R}) \qquad (4.4.4)$$

Substituting (4.4.4) into (4.4.3) and using orthonormality of the ϕs and the fact that σ_{Zi} is the Pauli spin operator for the ith electron, the N-body spin density becomes :

$$S(\underline{R}) = \left\{ \sum_{\text{Spin up}} |\phi_i(\underline{R})|^2 - \sum_{\text{Spin down}} |\phi(\underline{R})|^2 \right\}$$

$$S(\underline{R}) = \{ \sum_{\substack{\text{spin} \\ \text{up}}} |\emptyset(\underline{R})|^2 - \sum_{\substack{\text{spin} \\ \text{down}}} |\emptyset(\underline{R})|^2 \} \qquad (4.4.5)$$

The self-consistent solution of the defect cluster produces a set of Øs from which $S(\underline{R})$ can be calculated. We have written a subroutine for spin-density calculation along the lines suggested by Kung[Kung 81]. The value of the isotropic hyperfine constant is then completely determined by equation (4.4.2), and the results are listed in Table 4.13.

The F^+ center in MgO crystal was first identified by Wertz et al.[WAWS 57] through its electron spin resonance(ESR) spectrum. The ESR spectrum consists of an intense 'free-electron' absorption due to the F^+-center electrons interacting with only non-magnetic nuclei, and a number of weaker but fairly well-resolved hyperfine satellites from centers with one or more Mg^{25} isotopes (10.1% abundant, I=5/2) in <100> nearest-neighbor sites adjoining the vacancy. Unruh and Culvahouse[UC 67] in an electron-nuclear double-resonance (ENDOR) experiment have extended these results and have obtained an improved values for the isotrpic constant(a/h = 11.03 + 0.02 MHz).

Commencing with Table 4.13, it can be seen that agreement with experiment gets progressively better as we improve the Mg^{2+} basis set and include lattice relaxation in our calculations. This is what we expected since the isotropic

constant(a/h) is sensitive to the chosen basis set. Also the relaxed-lattice configuration shows an outward relaxation of the nearest-neighbor Mg^{2+} ions which is consistent with the ENDOR experiment[UC 67]. The calculated value of (a/h) with our best Mg^{2+} basis set(Basis MGT) comes out to be 13.12 MHz in a configuration corresponding to outward relaxation (3%) of nearest-neighbor ions. Thus, it can be concluded that Basis MGT is an adequate basis set to represent Mg^{2+} ions in the ground state of the F^+ center for the purpose of the present calculations.

Now we include (110) O^{2-} ions as the Hartree-Fock ions in the defect cluster and associate them with the set, Basis OXT. When the nearest-neighbor ions are held at the perfect-lattice positions, the value of (a/h) comes out to be 21.24 MHz showing an increase in (a/h) with the addition of these O^{2-} ions in the cluster. This is what we expected since the calculation in the perfect-lattice configuration has shown an increase of about 13% in the charge density centered at the vacancy. However when we relax the lattice, (a/h) turns out to be 6.94 MHz, a surprisingly low value. A possible explanation for this substantial decrease in (a/h) with the lattice relaxation may be a stronger ion-size effect of (110) O^{2-} ions onto the F^+-center wavefunction. Recall that the F^+-center wavefunction is compact in the ground state and the extent of its effect on the neighboring Mg^{25} nucleus determines the value of (a/h). In the relaxed-

TABLE 4.13

Isotropic Hyperfine Constant (a/h) for the nearest-neighbor Mg^{25} of the F^+ center in MgO.

	perfect-lattice configuration	relaxed-lattice configuration
(i) $F^+(e)$ - Mg6 Cluster		
Basis MGA (3,3/3)	26.73 MHz	21.63 MHz
Basis MGR (3,3,1/3,1)	20.25 MHz	16.21 MHz
Basis MGT (6,6/3)	17.01 MHz	13.12 MHz
(ii) $F^+(e)$ - Mg6012 Cluster		
Basis MGT (6,6/3) Basis OXT (7,7/4)	21.24 MHz	6.94 MHz

note : The experimental value of (a/h) is reported to be 11.03 MHz.

lattice configuration, the O^{2-} ions move inwardly and therefore the F^+-center wavefunction becomes more compact than that in the perfect-lattice configuration. We also note here that the nearest-neighbor Mg^{2+} ions relaxes outwardly. Hence the cumulative effect of the relaxation reduces the extent of interaction of the F^+-center wavefunction with the Mg^{25} nucleus. This calculated interaction is now significantly less than that required to represent the observed hyperfine interaction in the ENDOR study, and thereby representing a low value of (a/h). We may therefore conclude that the details of the electronic structure of the F^+-center ground state are sensitive to the O^{2-} ions.

We now turn our attention to the unrelaxed excited state of the F^+ center in magnesium oxide.

4.5 UNRELAXED EXCITED STATE

For the unrelaxed excited state (UNRES), we use either shell model or the basis set(Basis MGR) to represent Mg^{2+} ions in our defect cluster and optimise the range of p-type vacancy-centered fuction, oriented along z-axis. The results are presented in Figure 4.4. Accordingly, the UNRES wavefunction becomes diffuse with the introduction of the ion-size effect for Mg^{2+} ions, contrary to our expectations. The optimised range of the p-type function comes out to be well-beyond the nearest-neighbor distance. Also the use of Basis Causa which represents Mg^{2+} core states adequately does not change the picture at all(Figure 4.4).

Figure 4.4 : Optimisation of the vacancy-centered basis function in the unrelaxed excited state ($F^+(e)$-Mg6 cluster).

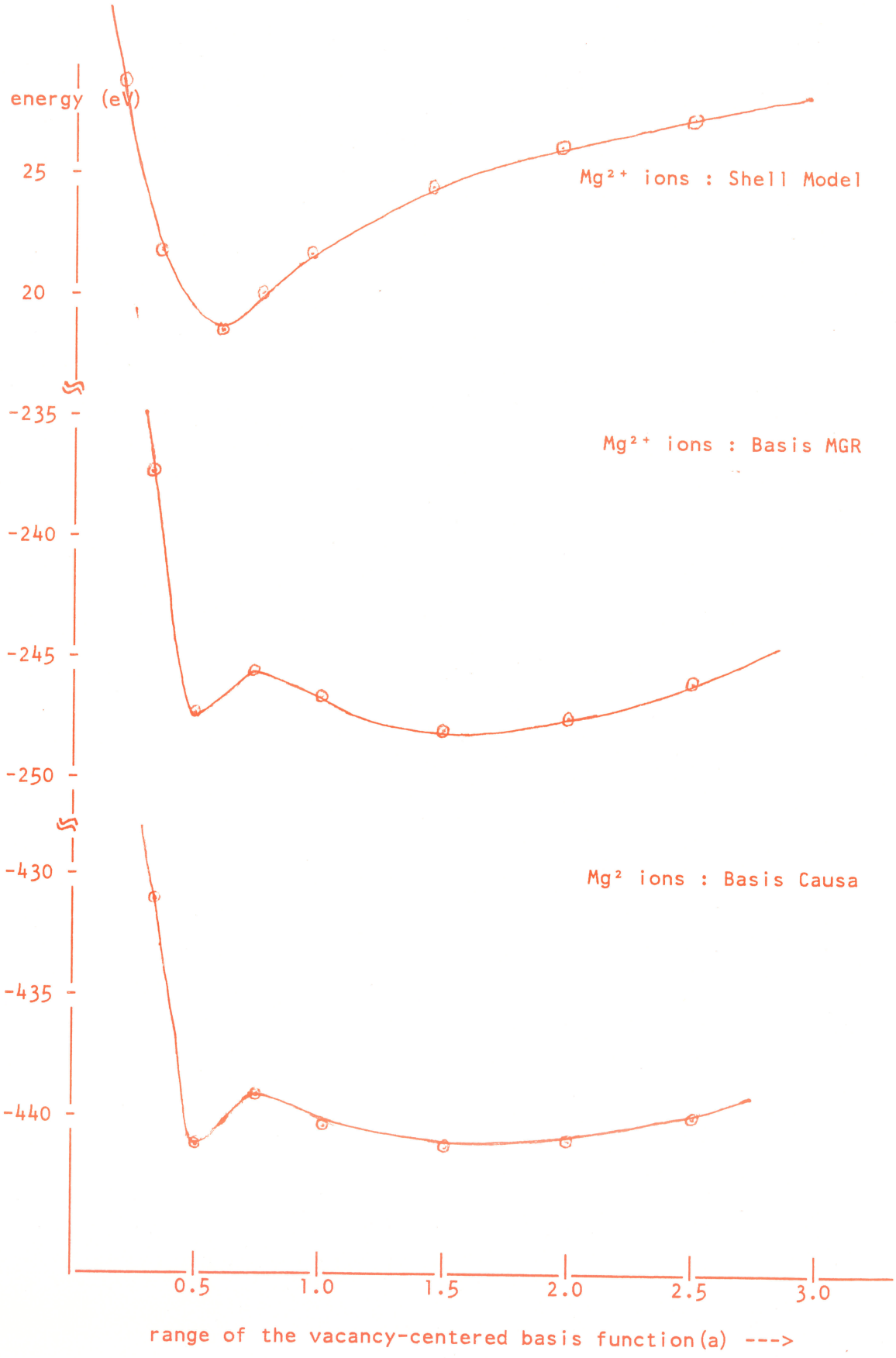
energy (eV)
25
20
-235
-240
-245
-250
-430
-435
-440
Mg²⁺ ions : Shell Model
Mg²⁺ ions : Basis MGR
Mg² ions : Basis Causa
0.5
1.0
1.5
2.0
2.5
3.0
range of the vacancy-centered basis function (a) --->

The diffuseness of the UNRES wavefunction may be an artifact of the absence of the ion-size effect of the second nearest-neighbor(110) O^{2-} ions of the vacancy. In our calculations, we have considered these O^{2-} ions as shell model ions which do not provide Pauli exclusion to the p-type vacancy-centered function. To verify this supposition, we now associate the Kunz-Klein localising potentials with second nearest-neighbor(110) O^{2-} ions, third nearest-neighbor(111) Mg^{2+} ions and fourth nearest-neighbor(200) O^{2-} ions and optimise the range of the UNRES wavefunction. The result is shown in Figure 4.5, indicating that the (weak) KKLP ion-size effect does not localise the UNRES wavefunction.

Now we replace KKLPs from (110) O^{2-} ions with Basis OXA in our cluster, expecting to provide a stronger ion-size effect to the UNRES wavefunction. It comes as no surprise that the UNRES wavefunction becomes localised with the optimised range of about 0.5a(Figure 4.5b). Thus, this calculation demonstrates that (110) O^{2-} ions play an important role in determining the excited state of the F^+ center and their ion-size effect must therefore be included in the defect cluster.

The absorption energy calculation constitutes our first test of the treatment of the unrelaxed excited state in the defect model. We therefore calculate absorption energy

Figure 4.5 : Optimisation of the vacancy-centered basis function in the unrelaxed excited state ($F^+(e)$-Mg_6O_{12} cluster)

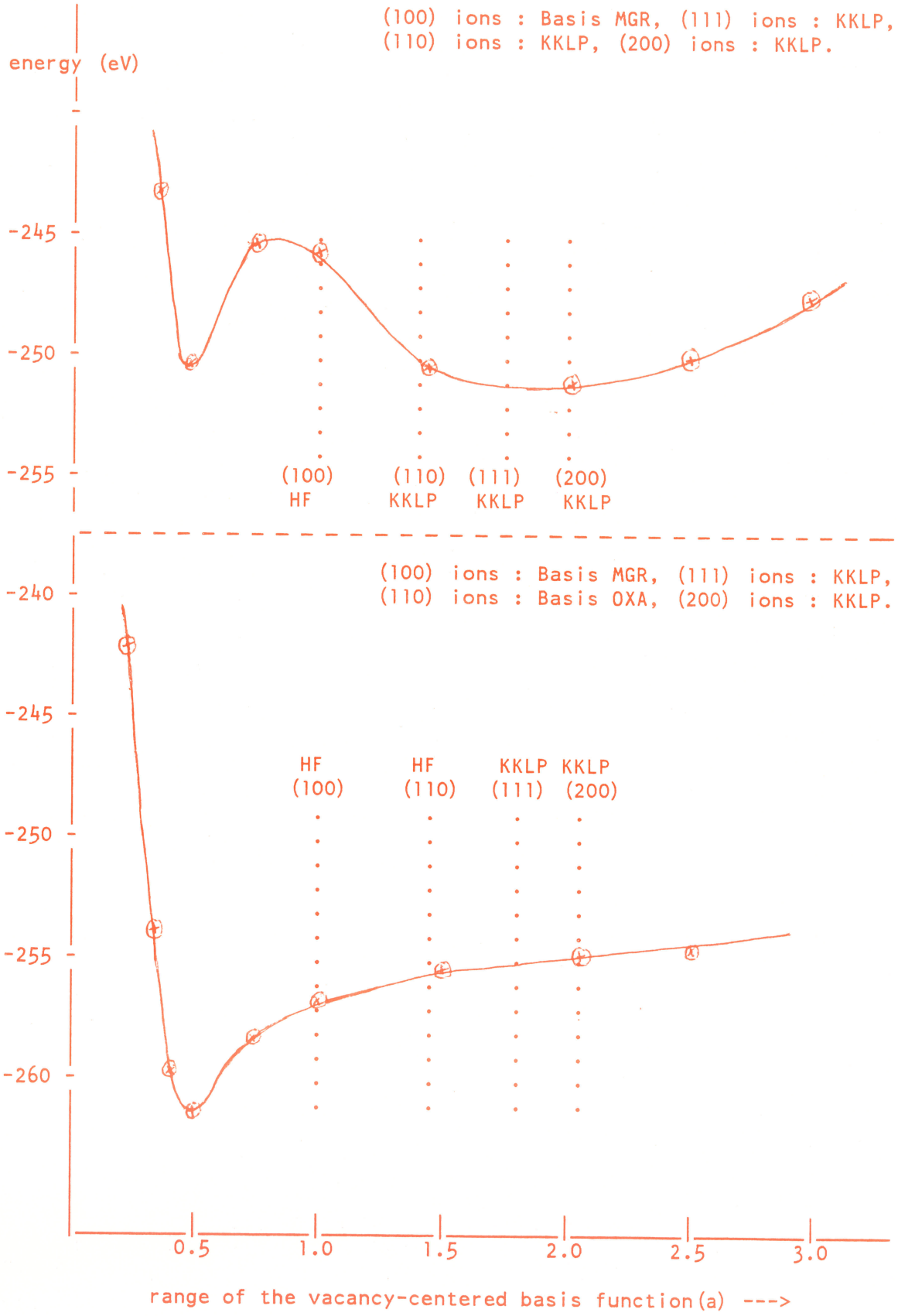
(100) ions : Basis MGR, (111) ions : KKLP,
(110) ions : KKLP, (200) ions : KKLP.
energy (eV)
-245
-250
-255
(100) HF
(110) KKLP
(111) KKLP
(200) KKLP
(100) ions : Basis MGR, (111) ions : KKLP,
(110) ions : Basis OXA, (200) ions : KKLP.
-240
-245
-250
-255
-260
HF (100)
HF (110)
KKLP (111)
KKLP (200)
0.5
1.0
1.5
2.0
2.5
3.0
range of the vacancy-centered basis function(a) --->

(which is the difference between the ground and unrelaxed excited state energies). The calculated result with Basis MGT/Basis OXT, our best Mg^{2+}/O^{2-} basis sets, is listed in Table 4.14. The absorption energy comes out to be 7.01 eV in comparison to the experimental value of 4.95 eV.

This failure of agreement seems to indicate the inadequacy of our model elements, particulary O^{2-} basis set for the unrelaxed excited state. Recall that Basis OXT is reoptimised in a perfect-lattice (non-defected) configuration. However, the (limited) available computational power prohibits us from doing optimisation of the O^{2-} basis set for the cluster in the unrelaxed excited state of the F^+ center. Furthermore, Mg^{2+} basis set(Basis MGT) employed in the unrelaxed excited state calculation is derived from the ground state calculation. But there may be fairly substantial readjustment of the electronic structure of these neighboring ions as the F^+ electron undergoes excitation from an s-like state to a p-like state. Hence it is of interest to optimise Mg^{2+} basis set in the unrelaxed excited state. Also, we have not taken account of either electron correlation or polaronic effect in any of the above calculations; although its effect may be small, it will be different for the ground and excited states, affecting the optical absorption energy.

TABLE 4.14

F^+-center : Absorption Energy

(F^+(e)-Mg6012 cluster)

Vacancy (000) / 1nn ions (100) / 2nn ions (110) / 3nn ions (111) / 4nn ions (200)	Basis FT / Basis MGT / Basis OXT / KKLP / KKLP	
	GS	UNRES
Absorption Energy	7.01 eV	
Vacancy- centered Basis : range	0.50a	0.50a
d(100)	1.03a	1.03a
d(110)	0.97a	0.97a
energy(eV)	-56535.08	-56528.07
RMS	0.85a	0.87a
Mulliken Population vacancy	1.0759	1.0644
(100) Mg^{2+} ion axial	9.9993	9.9972
planar	-	9.9999
(110) O^{2-} ion axial	9.9940	9.9929
planar	-	9.9995

Finally, the CPU time required for some of our calculations is given in Table 4.15 which should provide an idea of the magnitude of the computations involved.

4.6 CONCLUSION

The program package, ICECAP, offers a reliable method to perform localised electronic defect calculations in ionic crystals. We have tested its options and have examined its physical model using the defect, F^+ center in magnesium oxide.

The ground and unrelaxed excited states have been calculated. The F^+ center wavefunction in both the states is proven to be localised, as expected. The ground state is well-characterised, yielding a reliable value for the isotropic hyperfine constant. Spin density analysis qualitatively illustrates the importance of basis set optimisation of nearest-neighbor ions and self-consistent lattice relaxation for the ground state. The second nearest-neighbor O^{2-} ions play an important role in the optical absorption process, and must be included in the defect cluster describing the unrelaxed excited state of the F^+ center. The calculated absorption energy fails to agree with the experiment, probably due to inadequate basis set optimisation of near-neighbors in the unrelaxed excited state of the F^+ center.

TABLE 4.15

Amdahl 5870 CPU time required in one position iteration of ICECAP for some of the calculations reported here.

Cluster	number of electrons	number of basis functions	CPU time
$F^+(e)$	1	7	1 min
$F^+(e)$ + Mg6	61	31	12 min
$F^+(e)$ + Mg6	61	91	80 min
$F^+(e)$ + Mg6 + O12	181	91	380 min

By explicitly demonstrating the various steps in analysing the F^+-center ground state, it is hoped that this work will assist in yielding an adequate excited state when the computational power becomes available. It is also expected that the present work will serve as an example for further point-defect simulation studies, leading to reliable results where experimental data are less readily available.

Presently, ICECAP deals with a point-defect in an otherwise perfect, infinite ionic crystal. However, point-defect interactions with interfaces (surfaces,twins, and grain boundaries), and in finite crystals, as well as with dislocations are of technological importance and of fundamental interest. Since the UHF package has been successfully applied to a very wide range of condensed matter problems and Shell model treatments of most of these extended defects have been developed, the ICECAP code can therefore be extended to include these types of the defect in a crystalline lattice.

REFERENCES

Boys 50 — Boys,S.F., 1950, Proc.Roy.Soc.London, Ser A200, 542.

BO 27 — Born,M. and Oppenheimer,R., 1927, Ann.Phyk 84, 457.

BW 72 — Burden,F.R. and Wilson,R.M., 1972, Adv.in Phys. 21, 825.

BHS 82 — Bachelet,G.B., Hamann,D.R. and Schluter,M., 1982, Phys.Rev.B 28, 3465.

Cohe 84 — Cohen,M.L., 1984, Ann.Rev.Mat.Sci. 14, 119.

CA 80 — Ceperly,D.M. and Alder,B.A., 1980, Phys.Rev.Lett. 45, 566.

CN 73 — Catlow,C.R.A. and Norgett,M.J., 1973, J.Phys.C 6, 1325.

CR 74 — Clementi,E. and Roetti,C., 1974, Atomic Data and Nuclear Tables 14, 177.

CU 80 — Carsky,P. and Urban,M., 1980, Ab-initio calculations, (Springer, New York).

CDM 82 — Catlow,C.R.A., Dixon,M. and Mackrodt,W.C. in Computer Simulation of Solids, eds:C.R.A. Catlow and W.C.Mackrodt, 1982, p.130, (Springer, New York).

CKM 81 — Colbourn,E.A., Kendrick,J. and Mackrodt, W.C., 1981, ICI Laboratory Report, CL-R/81/1637/A.

CJMS 82 — Catlow,C.R.A., James,R., Mackrodt,W.C.and Stewart,R.F., 1982, Phys.Rev.B 25, 1006.

CDPR 86 — Causa,M., Dovesi,R., Pisani,C. and Roetti,C., 1986, Phys.Rev.B 33, 1308.

DO 58 — Dick,B.J. and Overhauser,A.W.,1958, Phys.Rev. 112, 90.

Flet 70 Fletcher,R., 1970, Comut.J. 13, 317.

Fock 30 Fock,V., 1930, Z.Physik 61, 126.

Gilb 64 Gilbert,T.L. in Molecular Orbitals in Chemistry, Physics and Biology, eds:P.O.Lowdin and B. Pullman, 1964, p.405, (Academic, New York).

Hark Harker,A.H., private communication.

Hart 28 Hartree,D.R., 1928, Proc.Cambridge Phil.Soc. 24, 89.

Hend 80 Henderson,B., 1980, CRC Critical Reviews in Solid State and Materials Science, 9, 1.

Huzi 84 Huzinaga S., 1984, Gaussians basis sets for molecular calculations, (Elsevier, Amsterdam).

HH 85 Harding,J.H. and Harker,A.H., 1985, Phil.Mag.B 51, 119.

HSC 79 Hamann,D.R., Schluter,M. and Chiang,C., 1979, Phys.Rev.Lett. 43, 1494.

HHK$^+$ 84 Harding,J.H., Harker,A.H., Keegstra,P.B., Pandey,R., Vail,J.M. and Woodward,C.W., 1984, Harwell report.

HRSP 86 Hehre,W.J., Radom,L., Schleyer,P., Popple,J., 1986, Ab Initio Molecular Orbital Theory, (Wiley, New York).

Keeg 86 Keegstra,P.B., 1986, Ph.D.Thesis, University of Illinois at Urbana-Champaign(unpublished).

Koop 33 Koopman,T., 1933, Physica 1, 104.

Kung 81 Kung,A.Y.S., 1981, Ph.D.Thesis, University of Manitoba(unpublished).

Kunz Kunz,A.B., University of Illinois and Michigan Technological University(unpublished).

Kunz 83 Kunz,A.B., 1983, Phys.Rev.B 28, 3465.

KK 78 Kunz,A.B. and Klein,D.L., 1978, Phys.Rev.B 17, 4614.

KS 65 Kohn,W. and Sham,L.J., 1965, Phys.Rev. 140, A1133.

KV — Kunz,A.B. and Vail,J.M., submitted for publication.

Lowd 55 — Lowdin,P.O., 1955, Phys.Rev. 97, 1474
97, 1490
97, 1509.

LN 72 — Lidiard,A.B. and Nogett,M.J. in Computational Solid State Physics, eds:F.Herman, N.W. Dalton and T.R.Koehler, 1972, p.385, (Plenum, New York).

Mack 82 — Mackrodt,W.C. in Computer Simulation of Solids, eds:C.R.A.Catlow and W.C.Mackrodt, 1982, p.175, (Springer, New York).

Mull 32 — Mulliken,R.S., 1932, Phys.Rev. 41, 49.

Mull 55 — Mulliken,R.S., 1955, J.Chem.Phys. 23, 1833.

MG 74 — Melius,C.F. and Goddard III,W.A., 1974, Phys.Rev.A 10, 1528.

ML 38 — Mott,N.F. and Littleton,M.J., 1938, Trans.Faraday Soc. 34, 485.

MS 79 — Mackrodt,W.C. and Stewart,R.F., 1979, J.Phys.C 12, 5015.

MOG 74 — Melius,C.F., Olafson,B.D. and Goddard III, W.A., 1974, Chem.Phys.Lett. 28, 457.

Norg 74 — Norgett,M.J., 1974, Harwell report, AERE - R 7650.

Norg 77 — Norgett,M.J., 1977, Harwell report, AERE - M 2880.

NBK+ — Neumann,D.B., Basch,H., Kornegay,R.L., Snyder, L.S., Moskowitz,J., Hornback,C. and Liebmann,S., POLYATOM(version 2) QCPE 199, Indiana University, Bloomington, USA.

PK 59 — Philips,J.C. and Kleinman,L., 1959, Phys.Rev. 116, 287.

PZ 81 — Perdew,J. and Zunger,A., 1981, Phys.Rev.B 23, 5048.

Reit 55 — Reitz,J.R., 1955, Solid State Physics, eds: F.Seitz and D.Turnbull, Volume 1, (Academy, New York).

Root 60 Roothaan,C.C.J., 1960, Rev.Mod.Phys. 32, 179.

Sang 74 Sangster,M.J., 1974, J.Phys.Chem.Solids 35, 195.

Slat 30 Slater,J.C., 1930, Phys.Rev. 35, 210.

Slic 78 Slichter,C.P., 1978, Principle of Magnetic Resonance, (Springer, New York)

Ston 81 Stoneham,A.M., 1981, Harwell report, AERE-R9598.

Ston 75 Stoneham,A.M., 1975, Theory of Defects, (Clarendon, Oxford)

Ston 74 Stoneham,A.M., 1974, J.Phys.C 7, 2476.

SS 81 Sangster,M.L. and Stoneham,A.M., 1981, Phil.Mag.B 43, 597.

SS 82 Schluter,M. and Sham,L.J., 1982, Physics Today, 35, 35.

SW 68 Seidel,H. and Wolf,H.C. in Physics of Color Centers, eds:W.B.Fowler, 1968, p. (Academic, New York).

TM 81 Tennyson,J. and Murrel,J.N., 1981, Mol.Phys. 42, 297.

TMM 78 Topiol,S., Moskowitz,J.W. and Melius,C.F., 1978, J.Chem.Phys. 68, 2364.

TMM$^+$ 76 Topiol,S., Moskowitz,J.W., Melius,C.F., Newton,M.D. and Jafri,J., 1976, Courant Institute of Mathematical Sciences, Report C00-3077-105, New York University.

UC 67 Unruh,W.P. and Culvahouse,J.W., 1967, Phys.Rev. 154, 861.

Vail 85 Vail,J.M., 1985, Phil.Mag.B 57, 101.

Vail 82 Vail,J.M., 1982, Harwell report, AERE-M3265.

VP 86 Vail,J.M. and Pandey,R. in Computer-based microscopic description of the structure and properties of materials, eds:J.Broughton, W. Krakow and S.T.Pantelides, 1986, p.247.

VW Vail,J.M. and Woodward,C., submitted for publication.

VHHS 84 Vail,J.M., Harker,A.H., Harding,J.H.and Saul,P.,

1984, J.Phys.C 17, 3401.

Wede 67 Wedepohl,P.T., 1967, Proc.Phys.Soc. 92, 79.

Whit 66 Whitten,J.L., 1966, J.Chem.Phys. 44, 395.

Wood 85 Woodward,C., 1985, Ph.D.Thesis, University of Illinois at Urbana-Champaign(unpublished).

WAWS 57 Wertz,J.E., Auzins,P., Weeks,R.A. and Silsbee, R.H., 1957, Phys.Rev. 107, 1535.

WSWK 80 Wepfer,G.G., Surratt,G.T., Weidman,R.S.and Kunz,A.B., 1980, Phys.Rev.B 21, 2596.

```
>*****************************************************************

    This is a sample data set for a calculation on the ground
  state of the F  center in Magnesium Oxide.
  The quantum-mechanical cluster is made up of the vacancy,
  (100) Mg2  and (110) O2  ions. KKLPs are associated with
  (111) and (200) near-neighbors.

>*****************************************************************
>
>
TITLE : FCENTER : MG8O12 WITH KKLP : MG2+ 1.03,  O2- 0.87
>
DEBUG CALCFX VAROMC
>
SCALE 2.106 ANGSTROM
>
ACCURACY CRYSTAL 1.D-3
>
LATTICE
1 1 0
1 0 1
0 1 1
>
BASIS
O   0 0 0
MG 1 1 1
END
>
VACANCIES
O     0    0    0
MG    1    0    0
MG    0    1    0
MG    0    0    1
MG   -1    0    0
MG    0   -1    0
MG    0    0   -1
>
>       2NN POSITIONS
>
O     1    1    0
O     1   -1    0
O     1    0    1
O     1    0   -1
```

```
O    -1    0    1
O    -1    0   -1
O    -1    1    0
O    -1   -1    0
O     0    1    1
O     0    1   -1
O     0   -1    1
O     0   -1   -1
>
>       3NN POSITIONS
>
MG    1    1    1
MG    1   -1    1
MG    1    1   -1
MG    1   -1   -1
MG   -1    1    1
MG   -1    1   -1
MG   -1   -1    1
MG   -1   -1   -1
>
>       4NN POSITIONS
>
O     2    0    0
O    -2    0    0
O     0    2    0
O     0   -2    0
O     0    0    2
O     0    0   -2
>
INTERSTITIALS
>
FC         0      0      0            FCEN
MG       V(1.03)  V(0)   V(0)         MAGX
MG       V(0)   V(1.03)  V(0)         MAGY
MG       V(0)   V(0)   V(1.03)        MAGZ
MG       V(-1.03)  V(0)   V(0)        MAGX
MG       V(0) V(-1.03)  V(0)          MAGY
MG       V(0)   V(0) V(-1.03)         MAGZ
>
>       2NN POSITIONS
>
O        V(0.97)    V(0.97)    V(0)          OXY
O        V(0.97)    V(-0.97)   V(0)          OXY
O        V(0.97)    V(0)       V(0.97)       OXY
O        V(0.97)    V(0)       V(-0.97)      OXY
O        V(-0.97)   V(0)       V(0.97)       OXY
O        V(-0.97)   V(0)       V(-0.97)      OXY
O        V(-0.97)   V(0.97)     V(0)         OXY
O        V(-0.97)   V(-0.97)   V(0)          OXY
O        V(0)       V(0.97)    V(0.97)       OXY
O        V(0)       V(0.97)    V(-0.97)      OXY
O        V(0)       V(-0.97)   V(0.97)       OXY
O        V(0)       V(-0.97)   V(-0.97)      OXY
>
```

```
>       3NN POSITIONS
>
MGLP    1    1    1          -          LPMG   KKLP
MGLP    1   -1    1          -          LPMG   KKLP
MGLP    1    1   -1          -          LPMG   KKLP
MGLP    1   -1   -1          -          LPMG   KKLP
MGLP   -1    1    1          -          LPMG   KKLP
MGLP   -1    1   -1          -          LPMG   KKLP
MGLP   -1   -1    1          -          LPMG   KKLP
MGLP   -1   -1   -1          -          LPMG   KKLP
>
>       4NN POSITIONS
>
OLP     2    0    0          -          LPO   KKLP
OLP    -2    0    0          -          LPO   KKLP
OLP     0    2    0          -          LPO   KKLP
OLP     0   -2    0          -          LPO   KKLP
OLP     0    0    2          -          LPO   KKLP
OLP     0    0   -2          -          LPO   KKLP
>
END
>
ATOMS
>
FC       0    -1
MG      12    +2
MGLP     2    +2
O        8    -2   -2.81   46.125    16.0
OLP     -2    -2   -2.81   46.125    16.0
>
BUCKINGHAM
>
O       O        22764.3   0.1490   20.37
OLP     O        22764.3   0.1490   20.37
OLP     OLP      22764.3   0.1490   20.37
O       MG       1275.2    0.3012   0.0
OLP     MG       1275.2    0.3012   0.0
OLP     MGLP     1275.2    0.3012   0.0
O       MGLP     1275.2    0.3012   0.0
END
>
REGION ONE 100
REGION TWO 5.6
REGION   X 5.6
CUTOFF SHELL 1.6
CUTOFF SPRING 0.3
>
FREEZE NONE
INITIAL PERFECT
>
GTOS FCEN
          S     0.126     1.0
>
GTOS MAGX
```

```
     S       854.89097        0.022845
             98.727577        0.127542
             21.335201        0.187178
             28.128657        0.032911
             2.2951125        0.028823
             0.79975294      -0.011074
     S       854.89097       -0.010839
             98.727577       -0.066309
             21.335201       -0.114281
             28.128657       -0.051193
             2.2951125        0.379727
             0.79975294       0.301423
     X       23.805108        0.033577
            5.1165930       0.134761
            1.2313920       0.172058
     Y      23.805108        0.058927
            5.1165930       0.236805
            1.2313920       0.300990
     Z      23.805108        0.058927
            5.1165930       0.236805
            1.2313920       0.300990
GTOS MAGY
     S       854.89097        0.022845
             98.727577        0.127542
             21.335201        0.187178
             28.128657        0.032911
             2.2951125        0.028823
             0.79975294      -0.011074
     S       854.89097       -0.010839
             98.727577       -0.066309
             21.335201       -0.114281
             28.128657       -0.051193
             2.2951125        0.379727
             0.79975294       0.301423
     X      23.805108        0.058927
            5.1165930       0.236805
            1.2313920       0.300990
     Y      23.805108        0.033577
            5.1165930       0.134761
            1.2313920       0.172058
     Z      23.805108        0.058927
            5.1165930       0.236805
            1.2313920       0.300990
GTOS MAGZ
     S       854.89097        0.022845
             98.727577        0.127542
             21.335201        0.187178
             28.128657        0.032911
             2.2951125        0.028823
             0.79975294      -0.011074
     S       854.89097       -0.010839
             98.727577       -0.066309
             21.335201       -0.114281
             28.128657       -0.051193
```

```
              2.2951125        0.379727
              0.78975294       0.301423
      X      23.805108       0.058827
             5.1165930       0.238805
             1.2313920       0.300990
      Y      23.805108       0.058827
             5.1165930       0.238805
             1.2313920       0.300990
      Z      23.805108       0.033577
             5.1165930       0.134761
             1.2313920       0.172056
 END
 >
 >
 GTOS OXY
      S    821.63934          0.018970
          123.68182           0.133227
           27.666170          0.446412
            7.2995700         0.471820
           10.805980          0.052033
            0.81784           0.043176
            0.2800           -0.013178
      S    821.63834          -0.003853
          123.68182           -0.029757
           27.666170          -0.106846
            7.2995700         -0.117476
           10.805950          -0.074976
            0.81784            0.463203
            0.2800             0.637957
      X    17.750370       0.034474
            3.86468        0.190821
            1.04772        0.370858
            0.28           0.611384
      Y    17.750370       0.034474
            3.86468        0.190821
            1.04772        0.370858
            0.28           0.611384
      Z    17.750370       0.034474
            3.86468        0.190821
            1.04772        0.370858
            0.28           0.611384
 END
 >
 ELECTRONS 91   90
 >
 ACCURACY POLY 1.D-9 1.1
 ITERATIONS UHF 40
 ACCURACY UHF 1.D-1
 CONVERGE ENERGY
 SORT     ENERGY
 >
 MULTIPOLE QUADRUPOLE
 ACCURACY MULTIPOLE 1.D-00
 ITERATIONS MULTIPOLE 00
```

```
 >
 ITERATIONS POSITIONS 01
 ACCURACY POSITIONS 1.D-1
 >
 >
 KKLP
 LPMG
   12
 FITTED POTENTIAL FOR MG IN MGO(RUN5)
 EXP                  GAMMA                LEADING COEF
   0              1.85015190E+00      -1.09318344E+00
   0              5.05650923E+00      -8.03289585E+00
   0              1.38325757E+01      -1.89524274E+01
   0              4.24837273E+01      -3.51456354E+01
   0              1.36042171E+02      -7.33089792E+01
   0              4.59722693E+02      -1.51440315E+02
   0              1.71870811E+03      -3.21625215E+02
   0              7.18998723E+03      -6.97365042E+02
   0              2.76842961E+04      -1.10649447E+03
   0              1.00762365E+05      -2.88035174E+03
   0              3.99476949E+05      -2.36247032E+03
   0              1.58308273E+06      -2.10866884E+04
 >
 >
 KKLP
 LPO
   13
 FITTED POTENTIAL FOR O IN MGO(RUN5)
 EXP                  GAMMA                LEADING COEF
   0              2.21358128E-01      -2.03000832E-01
   0              5.42406770E-01      -1.36759072E+00
   0              1.43347317E+00      -4.22378335E+00
   0              3.84421742E+00      -8.22898805E+00
   0              1.10839258E+01      -1.88835778E+01
   0              3.47990905E+01      -3.49259463E+01
   0              1.18555522E+02      -7.49343987E+01
   0              4.32462440E+02      -1.80152538E+02
   0              1.77058577E+03      -3.39403918E+02
   0              6.84096226E+03      -6.02842959E+02
   0              2.82211482E+04      -1.56761218E+03
   0              9.99094677E+04      -9.19748673E+02
   0              4.01256452E+05      -1.08141808E+04
 >
 ENTER
 STOP
 /*
 >**************************************************************
 >
 >
 >  JCL for executing the program on Amdahl 5870 computer system.
 >
 >
 >**************************************************************
```

```
//VAIL JOB '0201,,T=400M,L=80,I=3000',MSGLEVEL=(1,1),CLASS=1
//JOBLIB DD DSN=VAIL.PROGRAM.LOAD,
//          VOL=SER=USER06,UNIT=DISK,DISP=SHR
//       DD DSN=SYS1.VFORTLIB,UNIT=3350,
//          VOL=SER=SYS002,DISP=SHR
//  EXEC PGM=SOURCE,REGION=4500K
/*ROUTE PRINT LOCAL
//*
//*--------------------------------------------------------------
//FT01F001  DD UNIT=DISK,
//             SPACE=(TRK,(10,10),RLSE),DCB=(RECFM=VBS,LRECL=80,
//             BLKSIZE=3200),DISP=(NEW,PASS)
//*
//*            Scratch file for UHPROP
//*--------------------------------------------------------------
//FT02F001  DD DSN=VAIL.TEST.FT02,VOL=SER=SYS110,UNIT=DISK,
//             DISP=SHR
//*
//*            Copy file for POLYIN
//*--------------------------------------------------------------
//FT03F001  DD DSN=VAIL.TEST.FT03,VOL=SER=SYSSHR,UNIT=DISK,
//             DISP=SHR
//*
//*            Output file from LABELS
//*--------------------------------------------------------------
//FT04F001  DD DSN=VAIL.TEST.FT04,VOL=SER=SYSMVS,UNIT=DISK,
//             DISP=SHR
//*
//*            Output file from POLYIN
//*--------------------------------------------------------------
//FT06F001  DD SYSOUT=A
//*
//*             Print (output) file
//*--------------------------------------------------------------
//FT07F001  DD SYSOUT=A,DCB=(LRECL=133,RECFM=FA)
//*
//*             Print (detailed output) file
//*--------------------------------------------------------------
//FT20F001  DD DSN=VAIL.TEST.FT20,VOL=SER=SYSMVS,UNIT=DISK,
//*             SPACE=(TRK,(50,50),RLSE),DCB=(DSORG=DA,RECFM=F,
//*             LRECL=2048,BLKSIZE=2048),DISP=(NEW,KEEP)
//             DISP=SHR
//*
//*            UHF eigenvectors
//*--------------------------------------------------------------
//FT30F001  DD UNIT=DISK,
//             SPACE=(TRK,(10,10),RLSE),DCB=(DSORG=DA,RECFM=F,
//             LRECL=320,BLKSIZE=320),DISP=(NEW,PASS)
//*
//*            UHF data for MBPT
//*--------------------------------------------------------------
//FT41F001  DD DSN=VAIL.TEST.FT41,VOL=SER=SYS110,UNIT=DISK,
//             DISP=SHR
//*
```

```
//*        Input data for CRYDFN
//*--------------------------------------------------------------
//FT42F001  DD DSN=VAIL.TEST.FT42,UNIT=DISK,VOL=SER=SYS110,
//*            SPACE=(TRK,(3,1),RLSE),DCB=(RECFM=VBS,LRECL=800,
//*            BLKSIZE=3204),DISP=(NEW,KEEP)
//             DISP=SHR
//*
//*        Summary of main calculation to date
//*--------------------------------------------------------------
//FT43F001  DD DSN=VAIL.TEST.FT43,UNIT=DISK,VOL=SER=SYS110,
//*            SPACE=(TRK,(10,10),RLSE),DCB=(RECFM=FB,LRECL=80,
//*            BLKSIZE=3200),DISP=(NEW,KEEP)
//             DISP=SHR
//*
//*        Input data for HADES
//*--------------------------------------------------------------
//FT44F001  DD DSN=VAIL.TEST.FT44,UNIT=DISK,VOL=SER=SYS110,
//             DISP=SHR
//*
//*       Symmetry and class information input to LABELS.
//*--------------------------------------------------------------
//FT45F001  DD DSN=VAIL.TEST.FT45,VOL=SER=SYS110,UNIT=DISK,
//             DISP=SHR
//*
//*         Input data for integration phase
//*--------------------------------------------------------------
//FT47F001  DD DSN=VAIL.TEST.FT47,VOL=SER=SYS110,UNIT=DISK,
//             DISP=SHR
//*
//*         Input data for UHF-SCF phase
//*--------------------------------------------------------------
//FT48F001  DD DSN=VAIL.TEST.FT48,VOL=SER=SYS110,UNIT=DISK,
//             DISP=SHR
//*
//*         INPUT data for UHF properties phase
//*--------------------------------------------------------------
//FT49F001  DD DSN=VAIL.TEST.FT49,VOL=SER=SYS110,UNIT=DISK,
//*            SPACE=(TRK,(10,10),RLSE),DCB=(RECFM=FB,LRECL=80,
//*            BLKSIZE=3200),DISP=(NEW,KEEP)
//             DISP=SHR
//*
//*          OUTPUT from UHF properties calculation (MULTIPOLES)
//*--------------------------------------------------------------
//FT05F001  DD *
//*                          Main input file
//*--------------------------------------------------------------
```